UNITED AIRCRAFT CORPORATION

United Aircraft Research Laboratories

EAST HARTFORD, CONNECTICUT

United Aircraft Research Laboratories

UNITED AIRCRAFT CORPORATION

EAST HARTFORD, CONNECTICUT

Report J-970850-7

A Method for the Determination of
Optimal Multiple-Impulse
Rendezvous Trajectories

Contract NAS8-24440

Final Report

Prepared for George C. Marshall Space Flight Center

REPORTED BY J. R. Doll

J. R. Doll

APPROVED BY F. W. Gobetz

F. W. Gobetz

DATE February 1970

NO. OF PAGES 51

COPY NO. ________

Report J-970850-7

A Method for the Determination of
Optimal Multiple-Impulse
Rendezvous Trajectories

TABLE OF CONTENTS

Report J-970850-7

A Method for the Determination of Optimal Multiple-Impulse Rendezvous Trajectories

Contract NAS8-24440
Final Report

SUMMARY

This report documents the development of a new method for calculating optimal time-fixed multiple-impulse rendezvous trajectories in a three-dimensional, inverse-square gravity field. The method consists of applying the finite-difference Newton-Raphson algorithm, extended to handle parameter optimization, to the nonlinear system of equations describing the optimum trajectory. In the problem formulation, the magnitudes and timing of the impulses are treated as parameters for optimization. The equations which describe Lawden's necessary conditions for an optimal impulsive trajectory are used to couple the parameters to the system of state and adjoint equations.

Two methods are investigated for generating starting solutions for the multiple-impulse trajectory optimization routine developed, namely, the variable-thrust solution and the two-impulse solution. Both methods are utilized successfully in various test cases, and results are presented documenting the validity of each.

CONCLUSIONS

1. The finite-difference Newton-Raphson algorithm may be utilized for the determination of optimal, multiple-impulse, time-fixed rendezvous trajectories given an appropriate starting solution.

2. Neither the two-impulse nor the variable-thrust starting solutions result in convergence to optimal multiple-impulse solutions for all cases; however, in general, one or the other will yield an optimal solution.

INTRODUCTION

The survey of impulsive transfer performed under NASA Contract NAS8-21091, "Impulsive Transfer Study" (Ref. 1), revealed that the subject of optimal time-fixed rendezvous remains virtually unexplored. While hundreds of papers and reports on impulsive trajectory problems have been published, only a handful deal with rendezvous, and most of these provide only numerical results for specific problems. Thus, optimal rendezvous by impulses, despite its importance in many phases of space flight, is a subject toward which basic research has not been adequately applied.

Some specific aspects of rendezvous between bodies in space have been thoroughly researched, e.g., terminal-phase rendezvous and the dynamics of docking. Solutions of the equations of relative motion to first and second order permit good understanding of these phases of the rendezvous problem. What is lacking is a thorough analysis of the general problem, which can be defined as follows:

> Given two bodies performing time-related orbital motion in an inverse-square field, what sequence and number of ballistic arcs must be employed to bring one body into a rendezvous condition with the other in a fixed time and with minimum expenditure of impulse?

It should be pointed out that, if time of flight is not important, rendezvous always reduces to orbit transfer, since an appropriate waiting period can always be chosen to arrive at optimal transfer conditions. Transfer to a nearby orbit can reduce this waiting period with little penalty in impulse, but it is clear that excessive time penalties may be imposed and that such maneuvers cannot be considered satisfactory for all rendezvous problems. The fact that no solution to the general problem has been achieved is not surprising considering its complexity. Even the corresponding case of orbit transfer (without rendezvous between specific bodies in the orbits) has not been solved in its general form, although considerable progress toward a solution has been made in recent years.

The most difficult feature of the rendezvous problem, as defined above, is the determination of the optimal number of impulses. If only two impulses are allowed, a numerical solution can be readily attained. Furthermore, two-impulse, fixed-time rendezvous is a determinate problem with unique solutions involving single ballistic transfer paths. However, when additional impulses are allowed en route, degrees of freedom are introduced. A criterion for selecting values for these free variables, e.g., minimum impulse, must then be assumed, and the solution which is optimal with respect to this criterion must then be sought.

Three basic approaches have already been developed and used to handle the nonlinear three-impulse rendezvous problem. Two of these methods, which are documented in Refs. 2 and 3, differ primarily in computational detail rather than in concept. In both cases, a starting solution is generated, and a search procedure is used to converge to the desired optimal solution.

The method of Ref. 3 starts with a two-impulse rendezvous as the input case, and improves on it by proceeding in the minimum-ΔV gradient direction (method of parallel tangents). Although the two-impulse start is sufficient for "normal" solutions, it cannot handle cases involving long durations or transfer angles beyond one revolution. When a good start is obtained, however, the gradient descent process is quite rapid.

The method developed in Ref. 2 provides starting solutions for any terminal conditions. In this case, an optimal variable-thrust solution is obtained first by an efficient method such as that described in Ref. 4, and its primer history is used to locate the timing of the intermediate impulse. The physical location of the impulse is then taken from the corresponding point on the low-thrust trajectory. Such starting solutions have been found to be very effective (Refs. 2, 5, and 6), although more time-consuming than a simple impulsive solution. However, when mass data are being generated, only one variable-thrust starting solution is required, since the three-impulse solution from the first case is always an ideal input for neighboring cases.

Another method which was reported independently in Refs. 7 and 8 makes use of primer vector theory (Ref. 9) in combination with a conjugate gradient computational scheme to converge to an optimal solution. The methods described in Refs. 7 and 8 are very similar. Both attempt direct convergence to optimal impulsive trajectories using necessary conditions for an extremum. This approach is different from that taken in Ref. 2 wherein a variable-thrust solution is sought before convergence is attempted. In fact, in Ref. 8, a variable-thrust solution was sought using the impulsive solution as a starting guess.

The method developed herein also makes use of primer vector theory, but departs from Refs. 7 and 8 in that a Newton-Raphson technique is employed in the solution of the equation set. A drawback of the other techniques has been their exclusive use of two-impulse primer solutions to initiate the numerical optimization procedure. In the present method a variable-thrust primer is used as a starting solution when the two-impulse solution is clearly not even a neighboring solution to the optimum.

DISCUSSION

Problem Statement

The objective of this study is to devise a method and develop a numerical procedure for calculating optimum, time-fixed, multiple-impulse rendezvous trajectories. The general problem may be defined as follows:

Given two bodies performing time-related orbital motion in an inverse-square gravity field, what sequence and number of ballistic arcs must be employed to bring one body into a rendezvous condition, i.e., a matching of position and velocity, with the other in a fixed time and with minimum expenditure of impulse?

Analysis

An n-impulse trajectory is a sequence of coasting arcs, in an inverse-square potential field, joined together at points (impulses) in the trajectory where the velocity goes through a finite discontinuity. In cartesian coordinates, with the time unit appropriately chosen, the equations of motion of a body in a coasting arc are

$$\dot{x}_i = u_i \qquad i = 1,2,3 \tag{1}$$

and

$$\dot{u}_i = - x_i/r^3 \qquad i = 1,2,3\,, \tag{2}$$

where $r^2 = \sum_{i=1}^{3} x_i^2$.

The Euler-Lagrange equations are determined from the variational Hamiltonian

$$H = \sum_{i=1}^{3} \left[\nu_i u_i - \lambda_i x_i/r^3\right],$$

where ν_i and λ_i are Lagrange multipliers. These may be written as

$$\dot{\lambda}_i = - \frac{\partial H}{\partial u_i} = - \nu_i \tag{3}$$

$$\dot{\nu}_i = - \frac{\partial H}{\partial x_i} = \frac{\lambda_i}{r^3} - \frac{3x_i}{r^5} \sum_{\ell=1}^{3} \lambda_\ell x_\ell\,. \tag{4}$$

Combining Eqs. (3) and (4) to eliminate ν_i gives

$$\ddot{\lambda}_i = \frac{1}{r^3}\left(\frac{3 x_i S}{r^3} - \lambda_i\right), \tag{5}$$

where $S = \sum_{i=1}^{3} \lambda_i x_i$, which are the Euler-Lagrange equations written in second-order canonical form. The adjoint variables, λ_i, are the cartesian components of the primer vector as defined by Lawden in Ref. 10. Equations (1) and (2) may be similarly combined to yield the equations of motion in second-order form.

$$\ddot{x}_i = -x_i/r^3 \tag{6}$$

For the fixed-time rendezvous problem, the boundary conditions are the known positions and velocities at the specified initial and final times:

$$\begin{aligned} x_i(t_0) &= \alpha_i \\ \dot{x}_i(t_0) &= \dot{\alpha}_i \\ x_i(t_f) &= \beta_i \\ \dot{x}_i(t_f) &= \dot{\beta}_i \end{aligned} \tag{7}$$

Lawden, Ref. 10, has derived necessary conditions for an optimal, impulsive trajectory based on analysis of the primer vector. According to Lawden, if impulsive thrusts are permitted, the following conditions must be satisfied over an optimal trajectory:

(a) The primer and its first time derivative must be continuous.

(b) Whenever the rocket motor is operative, the thrust must be aligned with the primer which must have a certain constant magnitude P.

(c) The magnitude, p, of the primer must not exceed P on any null-thrust arc.

(d) The first time derivative of the primer must be zero at all impulse points not coincident with the end points.

Utilizing the above conditions on the primer vector over an optimal trajectory, the direction, magnitude, position, and time of each impulse in an optimal, multiple-impulse trajectory may be determined from an analysis of the adjoint variables. Rewriting conditions (b) and (d) in concise mathematical form yields

$$p(t_K) = P \qquad K = 1, \ldots, n \tag{8}$$

$$\dot{p}(t_K) = 0 \qquad 2 \leq K \leq n-1 , \tag{9}$$

where P is an arbitrary constant which may be scaled to any convenient value, usually P = 1, and t_k is the time of the kth impulse on an n-impulse trajectory.

If an impulse occurs in mid-trajectory, both its magnitude, v_k, and time, t_k, must be determined, and Eqs. (8) and (9) provide two constraints for the two unknowns. If the impulse occurs on the boundary, only the magnitude is unknown and only Eq. (8) is required. The equations coupling Eqs. (8) and (9) to the system Eqs. (5) and (6) are the corner conditions of the variational calculus which may be written as

$$\dot{x}_i(t_K^-) + \frac{\lambda_i(t_K)}{p(t_K)} v_K = \dot{x}_i(t_K^+) , \tag{10}$$

where λ_i/p are the direction cosines of the impulse as implied by condition (b), and the notation t_k^- and t_k^+ refers to times just prior to and following the kth impulse, respectively.

At the boundaries, Eq. (10) reduces to

$$\begin{aligned} \dot{x}_i(t_0) &= \dot{\alpha}_i + \frac{\lambda_i(t_0)}{p(t_0)} v_1 \\ \dot{x}_i(t_f) &= \dot{\beta}_i - \frac{\lambda_i(t_f)}{p(t_f)} v_n \end{aligned} \tag{11}$$

assuming that the first impulse occurs at t_o and the nth impulse occurs at t_f, which is by no means necessary. For this study, however, terminal impulses are assumed. Further analysis would be required to extend the method to include terminal coast phases.

The system of Eqs. (5) through (11) represents a mathematical description of the optimal impulsive rendezvous problem; solution of this system would represent an optimal rendezvous trajectory. Lawden's condition (c) is not included in the formulation; however, satisfaction of this condition may be checked after achieving a solution. It is also used as a means for determining the need for additional impulses in the numerical procedure,and the condition is thereby satisfied by the computer program which was developed in the study.

Method of Solution

The equations to be solved consist of a system of nonlinear differential equations with separated boundary conditions and a set of constraints on the unknown variables serving to define the impulse magnitudes and times. These unknown variables are included in the system as parameters for optimization. Problems involving the simultaneous optimization of trajectories and associated parameters have been successfully solved (Ref. 11) using the finite-difference Newton-Raphson algorithm (Ref. 4). A brief description of this method appears in Appendix I.

Basically, the system defined by Eqs. (5) through (11) is discretized by using a fixed number of equally spaced mesh points in each arc. An n-impulse trajectory has n-1 arcs and n impulse times, t_k $(k = 1,..,n)$, each of which is associated with a mesh point, j_k. Defining $t_1 = t_o$, $t_n = t_f$, $j_1 = 1$, and letting $j_n = m$ be the total number of mesh points, the mesh spacing, h, can then be expressed for each arc as

$$h_K = (t_{K+1} - t_K)/(j_{K+1} - j_K) \qquad K = 1, \ldots, n-1 \; . \tag{12}$$

At any mesh point, j, the value of the independent variable is

$$t_j = t_K + (j - j_K)\, h_K \; , \tag{13}$$

where $j_k \le j \le j_{k+1}$. The differential system may now be reduced to a large system of nonlinear, algebraic equations suitable for solution using the Newton-Raphson method by introducing the mesh spacing defined above and utilizing suitable approximations for the derivatives in the system of equations.

Applying the standard three-point formula for the second derivative

$$\ddot{\theta}_j = \frac{\theta_{j-1} - 2\theta_j + \theta_{j+1}}{h^2} \tag{14}$$

to Eqs. (5) and (6) yields, upon rearrangement,

$$f_{i,j} = x_{i,j-1} + x_{i,j}\left(\frac{h_K^2}{r_j^3} - 2\right) + x_{i,j+1} = 0 \tag{15}$$

and

$$g_{i,j} = \lambda_{i,j-1} + \lambda_{i,j}\left(\frac{h_K^2}{r_j^3} - 2\right) + \lambda_{i,j+1} - \frac{3h_K^2 \; x_{i,j} S_j}{r_j^5} = 0 \; . \tag{16}$$

Clearly, Eqs. (15) and (16) apply only at interior points of each arc of the trajectory. To complete the system, similar equations must be written at the boundaries and at each interior impulse point. To achieve this end, the mesh is extended on each arc one point beyond each of its end points. The added points are called implicit points. In the procedure employed, difference equations are written in terms of the functional values at the implicit points, and the equations are combined in such a way as to eliminate these undefined points. The negative superscript, (-), is used to denote variables or functions on or to the right of an impulse point which are related to the arc to the left of the impulse point, and, similarly, the superscript (+) is used to relate variables to the arc to the right of the impulse point.

At the boundaries, Eq. (7) gives half of the needed equations at each mesh point

$$f_{i,1} = \alpha_i - x_{i,1} = 0 \tag{17}$$

$$f_{i,m} = \beta_i - x_{i,m} = 0 \tag{18}$$

Since no mesh spacing is defined outside the boundary, h is assumed to be the same on both sides. Writing Eq. (15) for $j = 1$ and $j = m$ yields equations which depend on x_i's which lie outside the trajectory. These x_i's may be eliminated by using the appropriate form of Eq. (11) with the derivative terms replaced by the central-difference formula

$$\dot{x}_j = \frac{x_{j+1} - x_{j-1}}{2h} \; . \tag{19}$$

Carrying out the algebra yields the remaining required equations at the boundaries

$$g_{i,1} = x_{i,1}\left(\frac{h_1^2}{2r_1^3} - 1\right) - h_1\left(\dot{\alpha}_i + \frac{\lambda_{i,1}}{\rho_1} v_1\right) + x_{i,2} = 0 \tag{20}$$

$$g_{i,m} = x_{i,m}\left(\frac{h_{n-1}^2}{2r_m^3} - 1\right) + h_{n-1}\left(\dot{\beta}_i - \frac{\lambda_{i,m}}{\rho_m} v_n\right) + x_{i,m-1} = 0 \tag{21}$$

The method used requires that the coefficient matrix of partial derivatives, developed in Appendix II, be nonsingular. Experience has shown that this may be accomplished by substituting Eq. (8) for p_1 in Eq. (20) before taking the partial derivatives.

Equations at the intermediate impulse points may be derived in a similar fashion. Equation (15) is written twice with $j = j_k$ ($k = 2,..,n - 1$), once for $h = h_k$ and once for $h = h_{k-1}$. The undefined x_i's in each equation, i.e., x^-_{i,j_k+1} and x^+_{i,j_k-1}, are then solved for and substituted into the finite-difference form of Eq. (10) which contains the same undefined x_i's. Carrying out the algebra, and simplifying, yields

$$f_{i,j_K} = u x_{i,j_K-1} - x_{i,j_K}\left(v - \frac{w}{2r_{j_K}^3}\right) + x_{i,j_K+1} - \frac{h_K \lambda_{i,j_K} v_K}{\rho_{j_K}} = 0\,, \tag{22}$$

where $u = h_k/h_{k-1}$, $v = u + 1$, and $w = h_k(h_k + h_{k-1})$. The remaining equations are developed in the same way from Eq. (16) and Lawden's condition (a) on the continuity of the first derivative of the primer. Expressed in finite-difference form, this condition states that

$$\frac{\lambda^-_{j_K+1} - \lambda_{j_K-1}}{2h_{K-1}} = \frac{\lambda_{j_K+1} - \lambda^+_{j_K-1}}{2h_K}\,. \tag{23}$$

This operation yields the desired equations

$$g_{i,j_K} = u\lambda_{i,j_K-1} - \lambda_{i,j_K}\left(v - \frac{w}{2r_{j_K}^3}\right) + \lambda_{i,j_K+1} - \frac{3w x_{i,j_K} S_{j_K}}{2r_{j_K}^3} = 0\,, \tag{24}$$

where u, v, and w are as defined previously (Eq. (22)).

To complete the system, one additional equation must be appended to the system for each of the unknown parameters. If the initial and final times are included as unknown parameters, although they are in fact known for the fixed-time rendezvous problem, an n-impulse trajectory has 2n unknown parameters, the times, t_k, and magnitudes, v_k, of the n impulses. For notational convenience, and to provide the flexibility to include nonfixed initial or final time at some later date, this is the approach followed. Therefore, 2n additional equations defining the unknown parameters must be developed.

Equations defining the initial and final times may be written directly for the fixed-time rendezvous problem as

$$
\begin{aligned}
T_1 &= t_1 - t_0 = 0 \\
T_n &= t_n - t_f = 0 ,
\end{aligned}
\tag{25}
$$

where t_0 and t_f are the known initial and final times, respectively, and t_1 and t_n are the times of the first and nth impulses, previously assumed to occur at the boundaries. The remaining 2n-2 parameter equations may be developed from Eqs. (8) and (9) expressed in finite-difference form.

Equations defining the unknown impulse magnitudes, v_k, may be written directly from Eq. (8) as

$$V_K = \left[\sum_{i=1}^{3} \lambda_{i,j_K}^2 \right]^{1/2} - 1 = 0, \tag{26}$$

where k = 1,...,n and P = 1. Notice that the equations constraining the v_k do not depend on v_k at all. The fact that the parameter constraints need not depend on the parameters explicitly is explained in the development of the method in Appendix I. Equations defining the interior impulse times, t_k, for k = 2,...,n - 1 are derived from Eq. (9). Equation (9) may be rewritten as

$$\sum_{i=1}^{3} \lambda_{i,j_K} \dot{\lambda}_{i,j_K} = 0 . \tag{27}$$

If the central-difference expression of Eq. (19) is used to approximate the first derivative in Eq. (27), the result is an expression which is correct to first order but does not account for the possibility of unequal mesh spacing on the two coasting arcs joined at the mesh point j_k. To account for this possibility, which is highly likely, a Taylor series expansion is written about the point j_k. Expanding forward from j_k, and truncating higher-order terms gives

$$\lambda_{i,j_K+1} = \lambda_{i,j_K} + h_K \dot{\lambda}_{ij_K} + \frac{h_K^2}{2!} \ddot{\lambda}_{i,j_K} . \tag{28}$$

A similar expression for λ_{i,j_k-1} may also be developed. If these two equations are then combined and solved for $\dot{\lambda}_{i,j_k}$, the following expression results

$$\dot{\lambda}_{ij_K} = \frac{1}{h_K + h_{K-1}} \left\{ (\lambda_{ij_K+1} - \lambda_{i,j_K-1}) + \ddot{\lambda}_{i,j_K} \left(\frac{h_{K-1}^2 - h_K^2}{2} \right) \right\} . \tag{29}$$

Using Eq. (29) in Eq. (27), and substituting for $\ddot{\lambda}_{i,j_k}$ directly from Eq. (5), gives the desired result. After simplifying, the result is

$$T_K = \sum_{i=1}^{3} \lambda_{i,j_K} (\lambda_{i,j_K+1} - \lambda_{i,j_K-1}) + \frac{h_{K-1}^2 - h_K^2}{2 r_{j_K}^3} \left[\frac{3 S_{j_K}^2}{r_{j_K}^2} - \sum_{i=1}^{3} \lambda_{i,j_K}^2 \right] = 0 \tag{30}$$

Equation (30) is applied for k = 2,...,n - 1. The above equations complete the system of nonlinear algebraic equations used to approximate the second-order differential system of equations and appended constraints previously derived. The equations needed for the Newton-Raphson method, along with the required expressions for the Newton-Raphson matrix coefficients, are summarized in Appendix II for the convenience of the reader.

Starting Solutions

It is appropriate to view both the functions which are the solution of the differential equations and the values which are the solution of the unknown parameters all as a single point in some function space. Under fairly general conditions, it is known that the Newton iteration will converge to the solution point from some domain of neighboring points. The computational work required to identify this domain is, for most practical problems, too great to be justified. Instead, a heuristic approach to obtaining initial guesses is taken, the justification for which is its success.

The first approach followed is patterned after the theory developed in Ref. 9, wherein Lion extended the significance of the primer vector to nonoptimal trajectories and developed criteria for the optimality of additional impulses based on an examination of the primer vector for the two-impulse solution. If the two-impulse primer is of the types illustrated in Figs. 1(a) or 1(b), then the two-impulse solution is optimal, and additional impulses permit no saving in ΔV. If the primer appears as in (c) or (d) of Fig. 1, the two-impulse solution is nonoptimal, i.e., it does not satisfy Lawden's conditions, specifically condition (c) and, according to the theory, additional impulses are required for optimality. These additional impulses are initially placed at the interior maxima of the primer, and the two-impulse solution is then used to start the multiple-impulse iteration. The primer history illustrated in Fig. 1(e) implies a terminal coast according to Lion's theory, while Fig. 1(f) illustrates a two-impulse primer history from which no information about the form of the optimal solution may be derived from the theory.

For the purpose of developing a numerical routine utilizing two-impulse starting solutions, the approach taken herein was to generate the two-impulse solution to the rendezvous problem, and then to apply additional impulses at all interior maximum points of the two-impulse primer exceeding P, which is scaled so that P = 1. This was done regardless of the shape of the primer; e.g., the primer histories of both Fig. 1(e) and 1(f) would imply the existence of an additional impulse, and an optimal three-impulse solution would be sought. One of the chief advantages of the two-impulse starting solution is that it is a solution of the differential equations, although it does not satisfy all the conditions of interest. This type of starting solution is very often in the domain of convergence of the desired solution. One of the main disadvantages of the two-impulse starting solution is that it generally does not represent a good approximation to a multiple-impulse solution in a long-time or long-transfer-angle problem. This fact is readily apparent from an examination of the trajectories illustrated in Fig. 2 which correspond to a 275-day Mars-Earth rendezvous leaving Mars on Julian Date 2437460. The three-impulse solution shown was generated using the method described in Ref. 2. It is clear from the disparity between the two trajectories that the two-impulse solution cannot be expected to be in the domain of convergence of the desired three-impulse solution. It was for this reason that an alternative starting solution was considered.

The second type of starting solution utilized is the variable-thrust solution to the rendezvous problem. The rationale behind this method is based on the low-thrust analog developed in Ref. 2. Briefly, it is based on observed qualitative similarities between the primer vector over an impulsive trajectory, and typical low-thrust acceleration histories. Figure 3 depicts some typical low-thrust acceleration histories. The curves apply to a fixed launch date with variable trip time. Generally speaking, for short transfer time, acceleration decreases to a minimum and then increases (Fig. 3a). As mission time is increased, additional peaks have been seen to occur in typical cases. Thus, in Fig. 3(b) a small interior peak appears at some longer transfer time and, if time is increased further, as in Fig. 3(c), this peak dominates the curve. In some cases, a double interior peak has been observed (Fig. 3(d)). The curves in Figs. 3(a) to 3(d) may be qualitatively compared to those illustrated in Figs. 1(a) to 1(d). Exploiting this qualitative observation, the variable-thrust solution is used as a starting solution for the impulsive problem, with impulses applied at the terminals and at all interior maximum points on the acceleration history. The starting solution for the adjoint variables is obtained from the cartesian components of the acceleration normalized to 1.0 at the initial mesh point.

Experience has indicated that multiple-impulse solutions are optimal for most cases where the variable-thrust acceleration exhibits an interior maximum, regardless of the magnitude of the maximum. Therefore, even though a qualitative comparison of Figs. 1(b) and 3(b) would indicate that a two-impulse solution was optimal, a three-impulse solution would be sought for any case of the form depicted in Fig. 3(b). The approach taken, then, is similar to that used with the two-impulse starting solutions; i.e., the variable-thrust solution is generated and used as a starting solution, with impulses placed at the terminals and at all points of interior maxima in the acceleration history.

One of the chief advantages of using the variable-thrust starting solution is the ability to handle cases involving long transfer angles, even those involving transfers greater than 360 deg. The main disadvantage is the fact that the variable-thrust solution does not satisfy the differential equations. Experience has indicated that the domain of convergence to the desired result is smaller when the starting solution does not satisfy the differential equations. Previous experience with the low-thrust analog has also indicated that the variable-thrust acceleration does not always exhibit interior maxima when the optimal impulsive solution consists of more than two impulses. Numerically, however, this problem is overcome by examining the primer history of any converged solution for interior maxima violating Lawden's condition (c) and applying additional impulses at all points where this occurs. In fact, this same approach is followed in the case where the two-impulse starting solution is used; therefore the final converged trajectory, if one is obtained, is optimal and satisfies all of Lawden's conditions.

RESULTS

The system of equations derived in the foregoing were coded for numerical solution using the finite-difference Newton-Raphson algorithm. Several test cases were run to check the validity of the method developed. To check out the routines, two cases with easily obtainable analytical solutions were run, using these known solutions as input to the routines. The Hohmann transfer, illustrated in Fig. 4, was run to check the method out on the less complicated two-impulse case first. The routine converged, or shut off, in two iterations with no change in the input starting solution. The primer magnitude history for this case is depicted in Fig. 5; notice that for this case $\dot{p} = 0$ at the terminals, which implies that the transfer is globally optimal, a well known result. Optimality here is with respect to the number of impulses, although in this case it is also known to be the absolute optimum. That more than one optimal solution may be found, each with a different number of impulses, is shown in Ref. 7. However, for practical purposes, the maximum number of impulses may generally be restricted to some reasonable number, thereby limiting the number of different solutions which must be sought.

Having checked the numerical routine on an analytically known two-impulse case, the next step was to validate the procedure for a known multiple-impulse case. The bielliptic transfer illustrated in Fig. 6 was selected. Here the optimum transfer would again be the Hohmann; however, for fixed-time rendezvous, where the time is selected to correspond to the bielliptic transfer time, and the appropriate boundary conditions are used, the bielliptic transfer should be optimal. The starting solution used for this case was determined by patching together the two known Hohmann transfers comprising the bielliptic transfer. Again, the routine converged in two iterations, thereby verifying the system equations for multiple-impulse trajectories. The primer magnitude history for this case is illustrated in Fig. 7. Again the primer indicates global optimality, another known result for fixed-time rendezvous.

These two test cases merely serve to indicate the stability of the coupled system of state and adjoint equations augmented by the parameter-defining equations. To check the routine's ability to converge to a solution from an approximate starting solution, several real cases were also run. The two starting methods used have already been discussed. Figure 8 illustrates an optimal three-impulse solution to a coplanar Earth-Mars rendezvous problem generated using a nonoptimum two-impulse solution. The orbits of Earth and Mars are not shown in the figure so that the differences between the optimal three-impulse solution and the two-impulse and variable-thrust solutions, which are shown in the figure, may be emphasized.

The primer histories for both the nonoptimal two-impulse and the optimal three-impulse solutions, and the variable-thrust acceleration history normalized to 1.0 at the initial time, are illustrated in Fig. 9. An examination of the two-impulse primer indicates the nonoptimality of the two-impulse solution. The three-impulse case converged from the nonoptimal two-impulse solution in four iterations using 200 mesh points. Although the differences between the two- and three-impulse solutions are not great, the three-impulse solution is optimal for this case. The difference in ΔV is negligible ($\approx 0.5\%$), but it is apparent from the two-impulse primer that the two-impulse solution is near optimal, and large benefits are not to be expected. An examination of the variable-thrust acceleration history in Fig. 9 indicates no interior peak; therefore, this starting solution could not be used for this case, which points out one of the drawbacks previously mentioned, i.e., that the variable-thrust acceleration history does not always indicate the true form of the optimal solution.

Previous experience with the Newton-Raphson algorithm applied to three-dimensional trajectory optimization problems has indicated strong convergence properties using coplanar starting solutions. This convergence was verified by using the nonoptimal coplanar two-impulse solution to the above problem to generate the optimal three-dimensional three-impulse solution. For this case, the method converged in five iterations, again using 200 mesh points. The out-of-plane components for this case, however, are small and the total increase in ΔV was approximately 1.5%.

To verify the variable-thrust starting method, a 200-day Mars-Earth rendezvous in which the variable-thrust acceleration was known to exhibit an interior maximum was run. The two- and three-impulse and variable-thrust trajectory solutions for this case are shown in Fig. 10, with the associated primer histories depicted in Fig. 11. Although the interior maximum on the normalized variable-thrust acceleration history in Fig. 11 is not very pronounced, it clearly indicates the need for an additional impulse. Also, examination of the two-impulse primer history indicates the nonoptimality of the two-impulse solution.

In seeking a multiple-impulse solution, the variable-thrust starting solution was first used for the impulsive routine, with the two-impulse ΔV's as starting values for the terminal ΔV's and a zero value for the interior ΔV. However, convergence to a solution was not achieved. Several other starting guesses for the ΔV parameter values were then tried, but with no success. Finally, the two-impulse starting solution was used in the routine, and convergence was achieved in nine iterations. Even using the actual solution values for the ΔV parameters, the variable-thrust starting solution failed to converge. Thus, all attempts to obtain convergence from the variable-thrust starting solution for this case failed and the optimal three-impulse trajectory and primer history shown in Figs. 10 and 11, respectively, were generated using the two-impulse starting solution.

Failure of the variable-thrust starting solution for this case, while not investigated in great depth, can probably be explained by an examination and comparison of the actual variable-thrust and three-impulse trajectories. While these trajectories appear to be neighboring trajectories in Fig. 10, an examination of the actual trajectory data indicate significant differences in the timing. This is illustrated in Fig. 10 by the points a and b. These points correspond to positions in the trajectories at the same time. The same type of behavior is also noticeable in the values of the primer vector components. The variable-thrust solution is, as previously stated, not a solution of the coupled state and adjoint equations for a body in a coasting arc, and the significant differences observed in the timing over the two trajectories indicate that the variable-thrust solution is not a sufficiently good approximation to the impulsive solution to obtain convergence to the desired result.

The next case tried was a coplanar 400-day circle-to-circle rendezvous with a total transfer angle of 270 deg. The optimum three-impulse solution for this case is shown in Fig. 12, again with the corresponding two-impulse and variable-thrust solutions. The primer histories for these three solutions are illustrated in Fig. 13. Examination of the normalized variable-thrust primer history indicates a more pronounced interior peak than was seen in Fig. 11. The two-impulse primer history for this case is of the type depicted in Fig. 1(f). Lion's theory on nonoptimal primer histories makes no predictions on the form of the optimal trajectory for this type. When the variable-thrust solution was used to start the Newton iteration for this case, convergence was obtained for all nonzero initial guesses for the ΔV parameter values. Experimentation with initial values for the ΔV's indicated that the best initial guess, in terms of the fewest iterations needed to converge to the solution, was obtained by setting the ΔV's equal to the mesh spacing parameter on the variable-thrust trajectory times the instantaneous value of the acceleration at the point of application of the ΔV. Using this method, convergence to the optimal three-impulse solution was obtained in seven iterations. This method of estimating the ΔV's for the variable-thrust starting solution was therefore automated in the routine. A comparison of the variable-thrust and three-impulse trajectory data showed a much better correspondence in the timing over the two trajectories than was observed for the previous case. It is also apparent from a comparison of the primer histories in Fig. 13 that the normalized variable-thrust acceleration history represents a good approximation to the optimal three-impulse primer history.

The nonoptimal two-impulse solution was also used as a starting solution. However, for this case, the method did not converge. While the two-impulse starting solution does represent a solution of the coupled state and adjoint system, with zero intermediate ΔV, it is apparently not a sufficiently good approximation to the actual solution. It is clear from Fig. 13 that the two-impulse primer bears no resemblance to the optimal three-impulse primer. An examination of the two- and three-impulse trajectory data again reveals significant differences in the timing over the two trajectories.

An analysis of the run times for all the computer runs made indicates a computing time of approximately 0.01-0.10 sec per mesh point for each iteration on the Univac 1108. For example, the three-impulse solution shown in Fig. 10, using 300 mesh points, required nine iterations to converge and 97 sec computing time, giving a timing factor for this case of 0.036 sec per mesh point iteration. This time is reported only to give an indication of the efficiency of the method, and should be considered as an upper bound on actual run times, since no effort was made to consider coding efficiency in this preliminary effort.

RECOMMENDATIONS FOR FURTHER STUDY

The results of the present study have indicated a number of problems which, in the author's opinion, warrant further investigation. Also, several worthwhile applications and extensions of the method developed herein warrant consideration for further study.

It is generally felt that, while the present effort has developed an excellent method for use in determining the optimal multiple-impulse solution to time-fixed rendezvous problems, it still remains to exercise the method to gain a better understanding of the conditions under which convergence may be achieved from the two starting solutions which have been examined. It is apparent from the results of the study that both starting methods have areas in which they may be successfully applied; however, further research is needed to define the regions of applicability of each. What is needed is a method of generating satisfactory starting solutions for the general time-fixed rendezvous problem. The problem of allowing terminal coast phases in the optimal solution also warrants further study, because it is to be expected that divergence may occur for cases in which the optimal trajectory consists of a multiple-impulse trajectory together with one or more terminal coast phases.

Although the current study solved the time-fixed rendezvous problem, the method could be extended to handle other impulsive problems of interest. For example, it would be desirable to be able to optimize the trip time, within some given range, for a rendezvous trajectory departing or arriving on some specified date. Another problem of interest which could be handled by the method is the flyby mission, either powered or unpowered, wherein the flyby time would be optimized. Still another problem of interest which could be handled by the method is the round-trip mission. Here the outbound and inbound trip times would be optimized for a fixed mission time; stopover time could be either fixed or optimized also.

There are many possible applications of the method in areas of current interest. Among them are: (1) interplanetary mission analysis, (2) Earth-orbital operations, (3) injection into orbit, and (4) lunar orbit operations. For example, it may be possible to design a transfer maneuver in lunar space which would optimally place the Apollo capsule into a polar orbit, thereby allowing for exploration of the polar regions of the moon with a minimum fuel expenditure, possibly within the existing fuel constraints of the vehicle. Any applications worthy of the method should, of course, be preceded by the development of a sophisticated user tool from the program developed for this study.

REFERENCES

1. Gobetz, F. W., and J. R. Doll: A Survey of Impulsive Trajectories, Contract NAS8-21091, Final Report. UA Research Laboratories Report G-910557-11, June 1968.

2. Doll, J. R., and F. W. Gobetz: Three-Impulse Interplanetary Rendezvous Trajectories. Proceedings of the Southeastern Symposium on Missiles and Aerospace Vehicle Sciences of AAS, Huntsville, Alabama, Vol. II, December 1966, pp. 55-1 to 55-14.

3. Willis, E. A.: Optimization of Double Conic Interplanetary Trajectories. NASA TN D-3184, January 1966.

4. Van Dine, C. P., W. R. Fimple, and T. N. Edelbaum: Application of a Finite-Difference Newton-Raphson Algorithm to a Problem of Low-Thrust Trajectory Optimization. Progress in Astronautics, Vol. 17, Academic Press, Inc., New York, 1966.

5. Doll, J. R.: Earth-Orbit Masses for Five-Impulse Mars Stopover Missions in 1980. Journal of Spacecraft and Rockets, Vol. 5, No. 5, May 1968, pp. 517-521.

6. Gobetz, F. W., and J. R. Doll: How to Open a Launch Window. AAS Paper No. 68-095, AAS/AIAA Astrodynamics Specialist Conference, Jackson, Wyoming, September 1968.

7. Jezewski, D. J.: A Method for Determining Optimal, Fixed-Time N-Impulse Trajectories between Arbitrarily Inclined Orbits. Paper No. AD30 presented at the XIXth IAF Congress, New York, October 1968.

8. Minkoff, M., and P. M. Lion: Optimal Multi-Impulse Trajectories. Paper No. AD143 presented at the XIXth IAF Congress, New York, October 1968.

9. Lion, P. M.: A Primer on the Primer. Second Compilation of Papers on Trajectory Analysis and Guidance Theory. NASA-ERC PM-67-21, January 1968.

10. Lawden, D. F.: Optimal Trajectories for Space Navigation. Butterworths, London, 1963.

11. Van Dine, C. P.: Extension of the Finite-Difference Newton-Raphson Algorithm to the Simultaneous Optimization of Trajectories and Associated Parameters. AIAA Paper No. 68-115, January 1968.

12. Fimple, W. R., and C. P. Van Dine: Low Thrust Guidance Study. Contract N^S8-20119. Final Report, UA Research Laboratories Report E-910350-11, July 1966.

13. Kantorovich, L. V., and G. P. Akilov: Functional Analysis in Normed Spaces. Pergamon Press, New York, 1964, Chapter XVIII.

LIST OF TEXT SYMBOLS

x	Position coordinate
u	Velocity component
ν	Lagrange multiplier on x
λ	Lagrange multiplier on u, primer vector component
r	Radius
p	Primer vector magnitude
α	Initial position coordinate
$\dot{\alpha}$	Initial velocity component
β	Final position coordinate
$\dot{\beta}$	Final velocity component
t	Time
v	Impulse magnitude
h	Mesh spacing parameter

<u>Subscript Notation</u>

i	Number of dimensions (2 or 3)
j	Mesh point ($j = 1,\ldots,m$)
k	Impulse ($k = 1,\ldots,n$)
l	Dummy subscript
j_k	Mesh point of kth impulse
o	Initial time
f	Final time

APPENDIX I

Finite-Difference Newton-Raphson Algorithm

This section gives a brief construction of the finite-difference Newton-Raphson algorithm for the numerical solution of systems of second-order ordinary differential equations with split boundary conditions and an unknown vector of auxiliary parameters defined by a set of constraining equations. A complete discussion of the method is found in Ref. 12.

The algorithm operates by reducing the problem to a sequence of large, but specially structured, algebraic systems of linear equations. Mathematically, this reduction can be viewed in two ways. First, at each of many mesh points chosen along the independent variable axis between the boundary points, the nonlinear, ordinary differential equations describing the two-point boundary value problem may be written as algebraic equations by substituting difference quotients for the derivative terms. These algebraic equations are, in general, nonlinear in the unknown dependent variables. The Newton-Raphson iteration can be applied to this system. Second, however, the entire solution of the differential equations can be considered as a point in function space. The generalized Newton-Raphson iteration is applied directly to the nonlinear differential equations with the result being a system of linear differential equations. In this system, the unknown variables are the corrections to be made to an approximate solution which appears as a known function on the right-hand side. The standard numerical technique for solving systems of linear two-point boundary equations is to substitute difference quotients for the derivatives and solve the resulting system of linear algebraic equations.

When viewed the second way, the fact that the linear system will be specially structured becomes more evident. The matrices involved in solving ordinary, linear, boundary value problems are of block tri-diagonal form. They bear a close relationship to the matrices which arise in the solution of linear partial differential equations, which have been extensively studied. From previous experience, they are known to be well conditioned when solved by a direct elimination method known as the Block Thomas algorithm. This method is a labor-saving and convenient way of applying Gauss elimination to a block tri-diagonal system.

Returning to the algorithm itself, theoretical studies (Ref. 13) indicate, and computational experience shows, that through its use solutions are very quickly and easily obtained. Given an initial approximation to the solution, no more than five to seven terms of the sequence of linear problems are needed. The usual terminology is that each sequential solution of the linear system is a Newton-Raphson iteration. Also, the fact that no logical decisions have to be made during the course of the iteration is of no small importance to the success of the method.

The user is concerned only with providing the algorithm with an initial approximation or starting solution which is within the domain of convergence of the solution and may completely ignore the workings of the algorithm itself.

This section considers the development of the finite-difference Newton-Raphson algorithm from the first, or discrete, viewpoint. Consider the system of equations

$$\ddot{U} = F\,(U,W) \tag{A-1}$$

where U is a 2m vector and W is a vector of unknown parameters, say, of dimension n, defined in the interval

$$t_o \le t \le t_f,$$

with boundary conditions

$$\begin{aligned} U_i\,(t_o) &= \alpha_i \\ \dot{U}_i\,(t_o) &= \dot{\alpha}_i \\ U_i\,(t_f) &= \beta_i \\ \dot{U}_i\,(t_f) &= \theta_i, \end{aligned} \tag{A-2}$$

where i = 1,...,m, and the n auxiliary constraints needed to complete the definition of the system are

$$g_\ell\,(U,\,W) = 0, \qquad 1 \le \ell \le n. \tag{A-3}$$

It is not necessary for the vectors U or W to be complete in Eqs. (A-1) and (A-3). In fact, Eq. (A-3) need not depend on W at all. That is, W may enter the system completely through Eq. (A-1). The only requirement is that the system be fully determined. If a fixed number of mesh points is now introduced in the interval, with equal spacing defined by

$$h = (t_f - t_o)/(N-1), \tag{A-4}$$

where N is the total number of mesh points, the problem may be reduced to finding the solution of a large system of simultaneous nonlinear algebraic equations by approximating the derivative terms in Eq. (A-1). At the interior points of the arc, the standard three-point formula gives

$$U_{j-1} - 2\,U_j + U_{j+1} = h^2\,F_j \qquad \text{(A-5)}$$

or

$$P_j\,(U_{j-1},\,U_j,\,U_{j+1},\,W,\,h) = 0 \qquad \text{(A-6)}$$

To complete the system for the two-point boundary value problem, similar equations must be written at the boundaries. To this end, the mesh is extended one point beyond the boundaries. The added points are called implicit points. The procedure is to write difference equations in terms of the functional values at the implicit points, and to then combine equations in such a way as to eliminate these unnecessary values. This is accomplished by combining Eqs. (A-2) and (A-5) written for $j = 1$ and N. Of course, appropriate approximations must be used for the first derivative terms in Eq. (A-2), usually central-difference or truncated Taylor series. This results in equations of the form

$$P_1\,(U_1,\,U_2,\,W,\,h) = 0 \qquad \text{(A-7)}$$

and

$$P_N\,(U_{N-1},\,U_N,\,W,\,h) = 0 \qquad \text{(A-8)}$$

If, as in the problem studied in this report, there are intermediate values of the independent variable defined in the region of interest which are to be included in the unknown parameter vector W for optimization, the procedure is to fix the mesh points at which these values occur, and define several mesh spacing parameters over the interval. For example, if there are k intermediate values of the independent variable to be determined, then define j_k as the mesh point at which the t_k occurs, and define the mesh spacing as

$$h_K = (t_K - t_{K-1})/(j_K - j_{K-1}). \qquad \text{(A-9)}$$

The mesh points j_k represent boundary points of the k + 1 arcs over which different mesh spacing has been used and, accordingly, system equations must also be written at these points. The procedure is similar to that used for the boundary points, and the result is equations of the form

$$P_{j_K} = (U_{j_K-1},\ U_{j_K},\ U_{j_K+1},\ W,\ h_{K-1},\ h_K). \tag{A-10}$$

The additional equations defining the unknown parameters may also be considered as a vector function and written as

$$G\ (U_1, \ldots, U_N,\ W) = 0. \tag{A-11}$$

The system defined by Eqs. (A-6) through (A-8), (A-10), and (A-11) is now seen to be a large system of simultaneous algebraic equations, where the unknowns are the values of the vector U at each mesh point and the parameter vector W. It is well known that systems of this type may be solved by the generalized Newton-Raphson method, given an appropriate starting solution.

All that remains to be done is to write down the linear system which must be solved at each iteration and to indicate the method of its solution. The partial derivatives of the vector functions are, of course, matrices, and the following definitions are used.

$$\begin{aligned}
A_j &= -\ \partial P_j/\partial U_{j-1} \\
B_j &= -\ \partial P_j/\partial U_j \\
C_j &= -\ \partial P_j/\partial U_{j+1} \\
D_j &= -\ \partial P_j/\partial W \\
Q_j &= -\ \partial G/\partial U_j \\
S\ &= -\ \partial G/\partial W
\end{aligned} \tag{A-12}$$

The minus signs simplify the following matrix equations. Defining the iterative increment to be added to each U_j as ΔU_j, each iteration is represented by the linear system below.

$$
\begin{bmatrix}
B_1 & C_1 & & & & & & & & D_1 \\
A_2 & B_2 & C_2 & & & & & & & D_2 \\
& & & \ddots & & & & & & \vdots \\
& & & A_j & B_j & C_j & & & & D_j \\
& & & & & & \ddots & & & \vdots \\
& & & & & & A_{N-1} & B_{N-1} & C_{N-1} & D_{N-1} \\
& & & & & & & A_N & B_N & D_N \\
Q_1 & Q_2 & \cdots & & Q_j & \cdots & & Q_{N-1} & Q_N & S
\end{bmatrix}
\begin{bmatrix}
\Delta U_1 \\ \Delta U_2 \\ \vdots \\ \Delta U_j \\ \vdots \\ \Delta U_{N-1} \\ \Delta U_N \\ \Delta W
\end{bmatrix}
=
\begin{bmatrix}
P_1 \\ P_2 \\ \vdots \\ P_j \\ \vdots \\ P_{N-1} \\ P_N \\ G
\end{bmatrix}
\tag{A-13}
$$

Note that both the coefficient matrix and the right-hand side are functions of the unknowns, U_j and W, and are evaluated at the best known values from the previous iteration. At the solution, the right-hand side goes to zero. Thus, the iterative increments also go to zero since the matrix is nonsingular. The iteration is stopped when the ΔU_j and ΔW, or the $\Delta U_j/U_j$ or $\Delta W/W$, are all less than a specified epsilon. The solution of Eq. (A-13) is found as follows: first, forward elimination,

$$
\begin{aligned}
W_1 &= B_1^{-1} C_1, \; X_1 = B_1^{-1} D^1, \; Y_1 = B_1^{-1} P_1 \\
W_j &= (B_j - A_j W_{j-1})^{-1} C_j \\
X_j &= (B_j - A_j W_{j-1})^{-1} (D_j - A_j X_{j-1}) \\
Y_j &= (B_j - A_j W_{j-1})^{-1} (P_j - A_j Y_{j-1}), \qquad 2 \le j \le N.
\end{aligned}
\tag{A-14}
$$

second, back substitution,

$$
\begin{aligned}
K_N &= X_N \ , \ H_N = Y_N \\
K_j &= X_j - W_j \ K_{j-1} \\
H_j &= Y_j - W_j \ H_{j-1} \ , \ N\text{-}1 \geq j \geq 1
\end{aligned}
\tag{A-15}
$$

third, evaluating ΔW,

$$
\Delta W = (S - \sum_{j=1}^{N} Q_j \ K_j)^{-1} \ (R - \sum_{j=1}^{N} Q_j \ H_j) \tag{A-16}
$$

and, finally, the ΔU_j,

$$
\Delta U_j = H_j - K_j \ \Delta W, \qquad 1 \leq j \leq N. \tag{A-17}
$$

In Eq. (A-14), considerable simplification can be made with the observation that most of the A_j's and C_j's are either negative identity matrices or diagonal matrices. The matrices to be inverted in Eq. (A-14) are very well conditioned and may be inverted without a search for pivoted elements. However, the inversion of Eq. (A-16) requires the usual row search pivot technique. It should be noticed, however, that the work involved in solving Eq. (A-13) increases only linearly with the addition of mesh points.

APPENDIX II

Compendium of Equations and Matrix Coefficients

The analytic expressions for the partial derivatives required for the Newton-Raphson algorithm are given in this section. The finite-difference form of the system equations previously developed in the text are repeated here for the convenience of the reader. The subscript notation is the same as that used in the text and is briefly summarized below.

Subscript Notation

$i = 1, \ldots,$ number of dimensions (2, or 3)
$j = 1, \ldots,$ number of mesh points (m)
$k = 1, \ldots,$ number of impulses (n)
$\ell =$ dummy subscript
$j_k =$ mesh point at which kth impulse occurs.

The general form of the matrices for the Newton-Raphson algorithm is given by

$$A_j = -\partial P_j / \partial U_{j-1}$$
$$B_j = -\partial P_j / \partial U_j$$
$$C_j = -\partial P_j / \partial U_{j+1}$$
$$D_j = -\partial P_j / \partial W$$
$$Q_j = -\partial G / \partial U_j$$
$$S = -\partial G / \partial W$$

where

$$P_j = \begin{bmatrix} f_{i,j} \\ g_{i,j} \end{bmatrix}, \quad U_j = \begin{bmatrix} x_{i,j} \\ \lambda_{i,j} \end{bmatrix}, \quad G = \left[\begin{pmatrix} T \\ V \end{pmatrix}_K \right],$$

and

$$W = \left[\begin{pmatrix} t \\ v \end{pmatrix}_K \right]$$

Using the above notation, the equations and matrix coefficients for the Newton-Raphson method are:

Initial Boundary

$$f_{i,1} = \alpha_i - x_{i,1} = 0$$

$$g_{i,1} = x_{i,1}\left(\frac{h_1^2}{2r_1^3} - 1\right) - h_1\left(\dot{\alpha}_i + \frac{\lambda_{i,\ell}}{P_1} v_1\right) + x_{i,2} = 0$$

A_1 = undefined

$$B_1 = -\partial P_1/\partial U_1$$

$$-\frac{\partial f_{i,1}}{\partial x_{\ell,1}} = \delta_{i,\ell}$$

$$-\frac{\partial f_{i,1}}{\partial \lambda_{\ell,1}} = 0$$

$$-\frac{\partial g_{i,1}}{\partial x_{\ell,1}} = \delta_{i,\ell}\left(1 - \frac{h_1^2}{2r_1^3}\right) + \frac{3}{2} h_1^2 \frac{x_{i,1}\, x_{\ell,1}}{r_1^5}$$

$$-\frac{\partial g_{i,1}}{\partial \lambda_{\ell,1}} = \delta_{i,\ell}\frac{h_1 v_1}{P_1}$$

$$C_1 = -\partial P_1/\partial U_2$$

$$-\frac{\partial f_{i,1}}{\partial x_{\ell,2}} = 0$$

$$-\frac{\partial f_{i,1}}{\partial \lambda_{\ell,2}} = 0$$

$$-\frac{\partial g_{i,1}}{\partial x_{\ell,2}} = -\delta_{i,\ell}$$

$$-\frac{\partial g_{i,1}}{\partial \lambda_{\ell,2}} = 0$$

$$D_1 = -\partial P_1/\partial W$$

$$-\frac{\partial f_{i,1}}{\partial t_\ell} = 0$$

$$-\frac{\partial f_{i,1}}{\partial v_\ell} = 0$$

$$-\frac{\partial g_{i,1}}{\partial t_\ell} = \left[\dot{\alpha}_i + \frac{\lambda_{i,1}}{p_1} v_1 - h_1 \frac{x_{i,1}}{r_1^3}\right]\left[\frac{\delta_{2,\ell} - \delta_{1,\ell}}{j_2 - j_1}\right]$$

$$-\frac{\partial g_{i,1}}{\partial v_\ell} = \delta_{1,\ell}\, h_1 \frac{\lambda_{i,1}}{p_1}$$

Final Boundary

$$f_{i,m} = \beta_i - x_{i,m} = 0$$

$$g_{i,m} = x_{i,m}\left(\frac{h_{n-1}^2}{2r_m^3} - 1\right) + h_{n-1}\left(\dot{\beta}_i - \frac{\lambda_{i,m}}{p_m} v_n\right) + x_{i,m-1} = 0$$

$$A_m = -\partial P_m/\partial U_{m-1}$$

$$-\frac{\partial f_{i,m}}{\partial x_{\ell,m-1}} = 0$$

$$-\frac{\partial f_{i,m}}{\partial \lambda_{\ell,m-1}} = 0$$

$$-\frac{\partial g_{i,m}}{\partial x_{\ell,m-1}} = -\delta_{i,\ell}$$

$$-\frac{\partial g_{i,m}}{\partial \lambda_{i,m-1}} = 0$$

$$B_m = -\partial P_m/\partial U_m$$

$$-\frac{\partial f_{i,m}}{\partial x_{\ell,m}} = \delta_{i,\ell}$$

$$-\frac{\partial f_{i,m}}{\partial \lambda_{\ell,m}} = 0$$

$$-\frac{\partial g_{i,m}}{\partial x_{\ell,m}} = \delta_{i,\ell}\left(1 - \frac{h_{n-1}^2}{2 r_m^3}\right) + \frac{3}{2}\,\frac{h_{n-1}^2 x_{i,m} x_{\ell,m}}{r_m^5}$$

$$-\frac{\partial g_{i,m}}{\partial \lambda_{\ell,m}} = \delta_{i,\ell}\,\frac{h_{n-1} v_n}{p_m} + h_{n-1}\,\frac{v_n\,\lambda_{i,m}\lambda_{\ell,m}}{p_m^3}$$

C_m = undefined

$D_m = -\partial P_m/\partial W$

$$-\frac{\partial f_{i,m}}{\partial t_\ell} = 0$$

$$-\frac{\partial f_{i,m}}{\partial v_\ell} = 0$$

$$-\frac{\partial g_{i,m}}{\partial t_\ell} = \left[-\dot{\beta}_i + \frac{\lambda_{i,m} v_n}{p_m} - h_{n-1}\frac{x_{i,m}}{r_m^3}\right]\left[\frac{\delta_{\ell,n} - \delta_{\ell,n-1}}{j_n - j_{n-1}}\right]$$

$$-\frac{\partial g_{i,m}}{\partial v_\ell} = \delta_{\ell,n}\, h_{n-1}\,\frac{\lambda_{i,m}}{p_m}$$

<u>General Mesh Point</u>

$$f_{i,j} = x_{i,j-1} + x_{i,j}\left(\frac{h_K^2}{r_j^3} - 2\right) + x_{i,j+1} = 0$$

$$g_{i,j} = \lambda_{i,j-1} + \lambda_{i,j}\left(\frac{h_K^2}{r_j^3} - 2\right) + \lambda_{i,j+1} - \frac{3h_K^2\, x_{i,j} S_j}{r_j^5} = 0$$

for

$$j_K < j < j_{K+1} \quad \text{and} \quad S_j = \sum_{\ell=1}^{NDIM} x_{\ell,j}\,\lambda_{\ell,j}$$

$A_j = -\partial P_j/\partial U_{j-1}$

$$-\frac{\partial f_{i,j}}{\partial x_{\ell,j-1}} = -\delta_{i,\ell}$$

$$-\frac{\partial f_{i,j}}{\partial \lambda_{\ell,j-1}} = 0$$

$$-\frac{\partial g_{i,j}}{\partial x_{\ell,j-1}} = 0$$

$$-\frac{\partial g_{i,j}}{\partial \lambda_{\ell,j-1}} = -\delta_{i,\ell}$$

$B_j = -\partial P_j / \partial U_j$

$$-\frac{\partial f_{i,j}}{\partial x_{\ell,j}} = \delta_{i,\ell}\left(2 - \frac{h_K^2}{r_j^3}\right) + \frac{3h_K^2\, x_{i,j}\, x_{\ell,j}}{r_j^5}$$

$$-\frac{\partial f_{i,j}}{\partial \lambda_{\ell,j}} = 0$$

$$-\frac{\partial g_{i,j}}{\partial x_{\ell,j}} = \frac{3h_K^2}{r_j^5}\left[\delta_{i,\ell} S_j + x_{i,j}\lambda_{\ell,j} + \lambda_{i,j} x_{\ell,j} - \frac{5x_{i,j}\, x_{\ell,j}\, S_j}{r_j^2}\right]$$

$$-\frac{\partial g_{i,j}}{\partial \lambda_{\ell,j}} = \delta_{i,\ell}\left(2 - \frac{h_K^2}{r_j^3}\right) + \frac{3h_K^2\, x_{i,j}\, x_{\ell,j}}{r_j^5}$$

$C_j = -\partial P_j / \partial U_{j+1}$

$$-\frac{\partial f_{i,j}}{\partial x_{\ell,j+1}} = -\delta_{i,\ell}$$

$$-\frac{\partial f_{i,j}}{\partial \lambda_{\ell,j+1}} = 0$$

$$-\frac{\partial g_{i,j}}{\partial x_{\ell,j+1}} = 0$$

$$-\frac{\partial g_{i,j}}{\partial \lambda_{\ell,j+1}} = -\delta_{i,\ell}$$

$D_j = -\partial P_j / \partial W$

$$-\frac{\partial f_{i,j}}{\partial t_\ell} = \left[-\frac{2h_K\, x_{i,j}}{r_j^3}\right]\left[\frac{\delta_{\ell,K+1} - \delta_{\ell,K}}{j_{K+1} - j_K}\right]$$

$$-\frac{\partial f_{i,j}}{\partial v_\ell} = 0$$

$$-\frac{\partial g_{i,j}}{\partial t_\ell} = \frac{2h_K}{r_j^{\,3}}\left[\frac{3x_{i,j}S_j}{r_j^{\,2}} - \lambda_{i,j}\right]\left[\frac{\delta_{\ell,K+1}-\delta_{\ell,K}}{j_{K+1}-j_K}\right]$$

$$-\frac{\partial g_{i,j}}{\partial v_\ell} = 0$$

Interior Impulse Point

$$f_{i,j_K} = u x_{i,j_K-1} - x_{i,j_K}\left(v - \frac{w}{2r_{j_K}^3}\right) + x_{i,j_K+1} - \frac{h_K\lambda_{i,j_K}v_K}{p_{j_K}} = 0$$

$$g_{i,j_K} = u\lambda_{i,j_K-1} - \lambda_{i,j_K}\left(v - \frac{w}{2r_{j_K}^3}\right) + \lambda_{i,j_K+1} - \frac{3w x_{i,j_K}S_{j_K}}{2r_{j_K}^3} = 0$$

where $u = h_K/h_{K-1}$, $v = u+1$ and $w = h_K(h_K + h_{K-1})$

$$A_{j_K} = -\partial P_{j_K}/\partial U_{j_K-1}$$

$$-\frac{\partial f_{i,j_K}}{\partial x_{\ell,j_K-1}} = -\delta_{i,\ell}\,u$$

$$-\frac{\partial f_{i,j_K}}{\partial \lambda_{\ell,j_K-1}} = 0$$

$$-\frac{\partial g_{i,j_K}}{\partial x_{i,j_K-1}} = 0$$

$$-\frac{\partial g_{i,j_K}}{\partial \lambda_{\ell,j_K-1}} = -\delta_{i,\ell}\,u$$

$$B_{j_K} = -\partial P_{j_K}/\partial U_{j_K}$$

$$-\frac{\partial f_{i,j_K}}{\partial x_{\ell,j_K}} = \delta_{i,\ell}\left(v - \frac{w}{2r_{j_K}^3}\right) + \frac{3w x_{i,j_K}x_{\ell,j_K}}{2r_{j_K}^5}$$

$$-\frac{\partial f_{i,j_K}}{\partial \lambda_{\ell,j_K}} = \frac{h_K v_K}{p_{j_K}}\left[\delta_{i,\ell} - \frac{\lambda_{i,j_K}\lambda_{\ell,j_K}}{p^2_{j_K}}\right]$$

$$-\frac{\partial g_{i,j_K}}{\partial x_{\ell,j_K}} = \frac{3w}{2r^3_{j_K}}\left[\delta_{i,\ell} S_{j_K} + x_{i,j_K}\lambda_{\ell,j_K} + \frac{\lambda_{i,j_K} x_{\ell,j_K}}{r^2_{j_K}} - \frac{3x_{i,j_K} x_{\ell,j_K} S_{j_K}}{r^2_{j_K}}\right]$$

$$-\frac{\partial g_{i,j_K}}{\partial \lambda_{\ell,j_K}} = \delta_{i,\ell}\left(v - \frac{w}{2r^3_{j_K}}\right) + \frac{3wx_{i,j_K} x_{\ell,j_K}}{2r^5_{j_K}}$$

$$C_{j_K} = -\partial P_{j_K}/\partial U_{j_K+1}$$

$$-\frac{\partial f_{i,j_K}}{\partial x_{\ell,j_K+1}} = -\delta_{i,\ell}$$

$$-\frac{\partial f_{i,j_K}}{\partial \lambda_{\ell,j_K+1}} = 0$$

$$-\frac{\partial g_{i,j_K}}{\partial x_{\ell,j_K+1}} = 0$$

$$-\frac{\partial g_{i,j_K}}{\partial \lambda_{\ell,j_K+1}} = -\delta_{i,\ell}$$

$$D_{j_K} = -\partial P_{j_K}/\partial W$$

$$-\frac{\partial f_{i,j_K}}{\partial t_\ell} = \left[\frac{\lambda_{i,j_K} v_K}{p_{j_K}} + \frac{x_{i,j_K} - x_{i,j_K-1}}{h_{K-1}} - \frac{x_{i,j_K}}{2r_{j_K}{}^3}\left(2h_K + h_{K-1}\right)\right]\left[\frac{\delta_{K+1,\ell} - \delta_{K,\ell}}{j_{K+1} - j_K}\right]$$

$$+\left[\frac{u}{h_{K-1}}\left(x_{i,j_K-1} - x_{i,j_K}\right) - \frac{x_{i,j_K}}{2r_{j_K}{}^3} h_K\right]\left[\frac{\delta_{K,\ell} - \delta_{K-1,\ell}}{j_K - j_{K-1}}\right]$$

$$-\frac{\partial f_{i,j_K}}{\partial v_\ell} = \delta_{K,\ell}\frac{h_K \lambda_{i,j_K}}{p_{j_K}}$$

$$-\frac{\partial g_{i,j_K}}{\partial t_\ell} = \left[\frac{\lambda_{i,j_K} - \lambda_{i,j_K-1}}{h_{K-1}} + \left(2h_K + h_{K-1}\right)\left(\frac{3x_{i,j_K} S_{j_K} - \lambda_{i,j_K}}{2r_{j_K}{}^3}\right)\right]\left[\frac{\delta_{K+1,\ell} - \delta_{K,\ell}}{j_{K+1} - j_K}\right]$$

$$+\left[\frac{h_K}{h_{K-1}{}^2}\left(\lambda_{i,j_K-1} - \lambda_{i,j_K}\right) + \frac{h_K}{2r_{j_K}{}^3}\left(3x_{i,j_K} S_{j_K} - \lambda_{i,j_K}\right)\right]\left[\frac{\delta_{K,\ell} - \delta_{K-1,\ell}}{j_K - j_{K-1}}\right]$$

$$-\frac{\partial g_{i,j_K}}{\partial v_\ell} = 0$$

Parameter Equations

$$T_1 = t_1 - t_0 = 0$$

$$V_1 = \left[\sum_{i=1}^{3} \lambda_{i,1}^2\right]^{1/2} - 1 = 0$$

$$\vdots$$

$$T_K = \sum_{i=1}^{3} \lambda_{i,j_K}\left(\lambda_{i,j_K+1} - \lambda_{i,j_K-1}\right) + \frac{h_{K-1}^2 - h_K^2}{2r_{j_K}^3}\left[\frac{3S_{j_K}^2}{r_{j_K}^2} - \sum_{i=1}^{3}\lambda_{i,j_K}^2\right] = 0$$

$$V_K = \left[\sum_{i=1}^{3} \lambda_{i,j_K}^2\right]^{1/2} - 1 = 0$$

$$\vdots$$

$$T_n = t_n - t_f = 0$$

$$V_n = \left[\sum_{i=1}^{3} \lambda_{i,j_n}^2\right]^{1/2} - 1 = 0$$

$$Q_j = -\partial G / \partial U_j$$

$$-\frac{\partial T_1}{\partial x_{\ell,j}} = 0$$

$$-\frac{\partial T_1}{\partial \lambda_{\ell,j}} = 0$$

$$-\frac{\partial V_1}{\partial x_{\ell,j}} = 0$$

$$-\frac{\partial V_1}{\partial \lambda_{\ell,j}} = -\delta_{j,1}\lambda_{\ell,j} \Big/ \left[\sum_{i=1}^{3}\lambda_{i,j}^2\right]^{1/2}$$

$$-\frac{\partial T_K}{\partial x_{\ell,j}} = -\frac{3\left(h_{K-1}^2 - h_K^2\right)}{2r_{j_K}^5}\left[2\lambda_{\ell,j_K}S_{j_K} - \frac{5S_{j_K}^2 x_{\ell,j_K}}{r_{j_K}^2} + x_{\ell,j_K}\sum\lambda_{i,j_K}^2\right]\delta_{j,j_K}$$

$$-\frac{\partial T_K}{\partial \lambda_{\ell,j}} = -\delta_{j,j_K}\left[\frac{\left(h_{K-1}^2 - h_K^2\right)}{r_{j_K}^3}\left(\frac{3S_{j_K}x_{\ell,j_K}}{r_{j_K}^2} - \lambda_{\ell,j_K}\right) + \left(\lambda_{\ell,j_K+1} - \lambda_{\ell,j_K-1}\right)\right]$$

$$-\lambda_{\ell,j_K}\left(\delta_{j,j_K+1} - \delta_{j,j_K-1}\right)$$

$$-\frac{\partial V_K}{\partial x_{\ell,j}} = 0$$

$$-\frac{\partial V_K}{\partial \lambda_{\ell,j}} = -\delta_{j,j_K}\, \lambda_{\ell,j} \Big/ \left[\sum_{i=1}^{3} \lambda_{i,j}^{2}\right]^{1/2}$$

$$-\frac{\partial T_n}{\partial x_{\ell,j}} = 0$$

$$-\frac{\partial T_n}{\partial \lambda_{\ell,j}} = 0$$

$$-\frac{\partial V_n}{\partial x_{\ell,j}} = 0$$

$$-\frac{\partial V_n}{\partial \lambda_{\ell,j}} = -\delta_{j,j_n}\, \lambda_{\ell,j} \Big/ \left[\sum_{i=1}^{3} \lambda_{ij}^{2}\right]^{1/2}$$

$$S = -\partial G/\partial W$$

$$-\frac{\partial T_1}{\partial t_\ell} = -\delta_{\ell,1}$$

$$-\frac{\partial T_1}{\partial v_\ell} = 0$$

$$-\frac{\partial V_1}{\partial t_\ell} = 0$$

$$-\frac{\partial V_1}{\partial v_\ell} = 0$$

$$-\frac{\partial T_K}{\partial t_\ell} = -\frac{1}{r_{j_K}^{3}} \left[\frac{3 S_{j_K}}{r_{j_K}^{2}} - \sum_{i=1}^{3} \lambda_{i,j_K}^{2}\right] \left[\frac{h_{K-1}}{j_K - j_{K-1}} \left(\delta_{K,\ell} - \delta_{K-1,\ell}\right) - \frac{h_K}{j_{K+1} - j_K} \left(\delta_{K+1,\ell} - \delta_{K\ell}\right)\right.$$

$$-\frac{\partial T_K}{\partial v_\ell} = 0$$

$$-\frac{\partial V_K}{\partial t_\ell} = 0$$

$$-\frac{\partial V_K}{\partial v_\ell} = 0$$

$$-\frac{\partial T_n}{\partial t_\ell} = -\delta_{\ell,n}$$

$$- \frac{\partial T_n}{\partial v_\ell} = 0$$

$$- \frac{\partial V_n}{\partial t_\ell} = 0$$

$$- \frac{\partial V_n}{\partial v_\ell} = 0$$

J-970850-7

FIG. 1

TYPICAL TWO-IMPULSE PRIMER HISTORIES

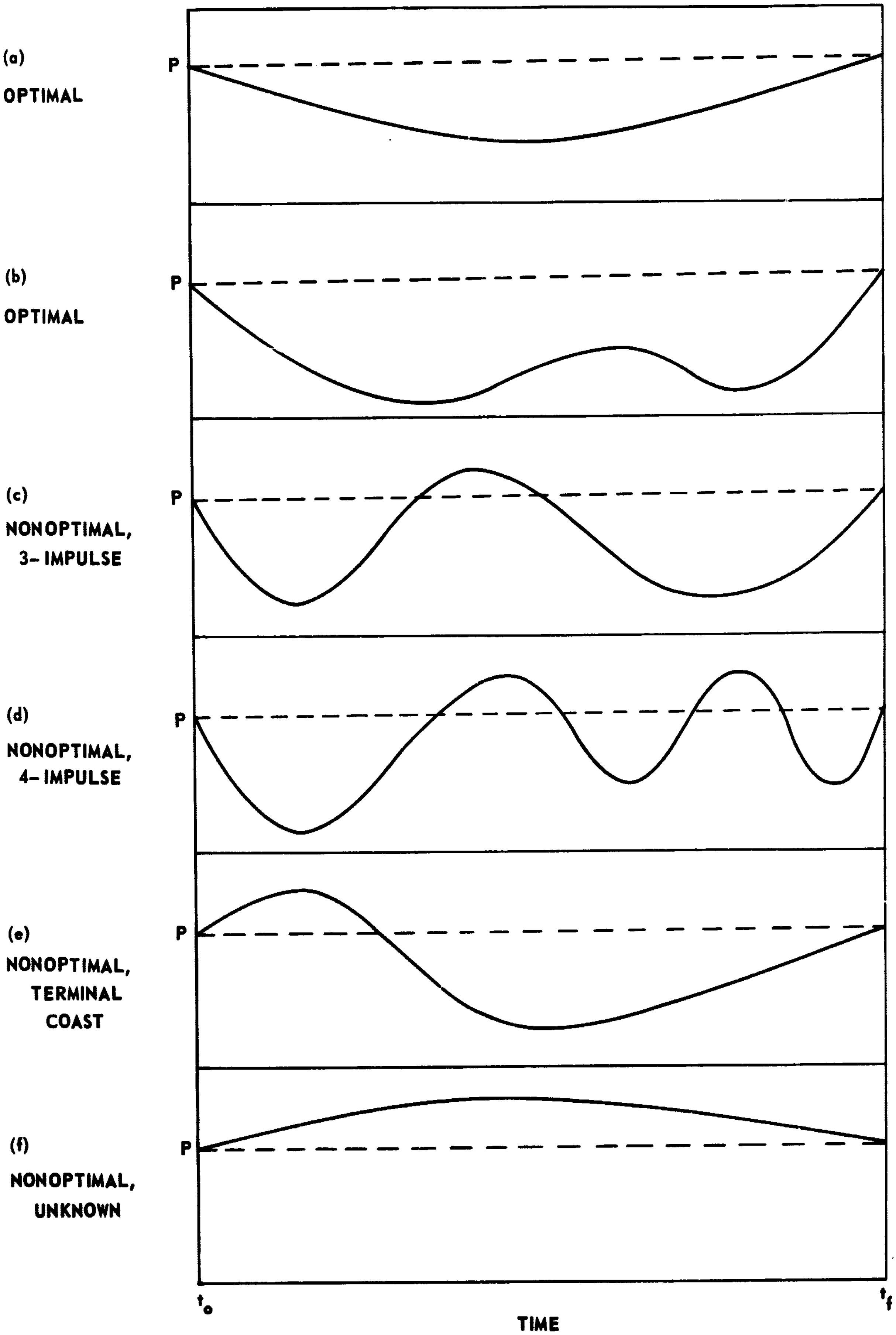

MARS–EARTH TRAJECTORIES

THREE IMPULSES

$\Delta V_T = 0.639$ EMOS

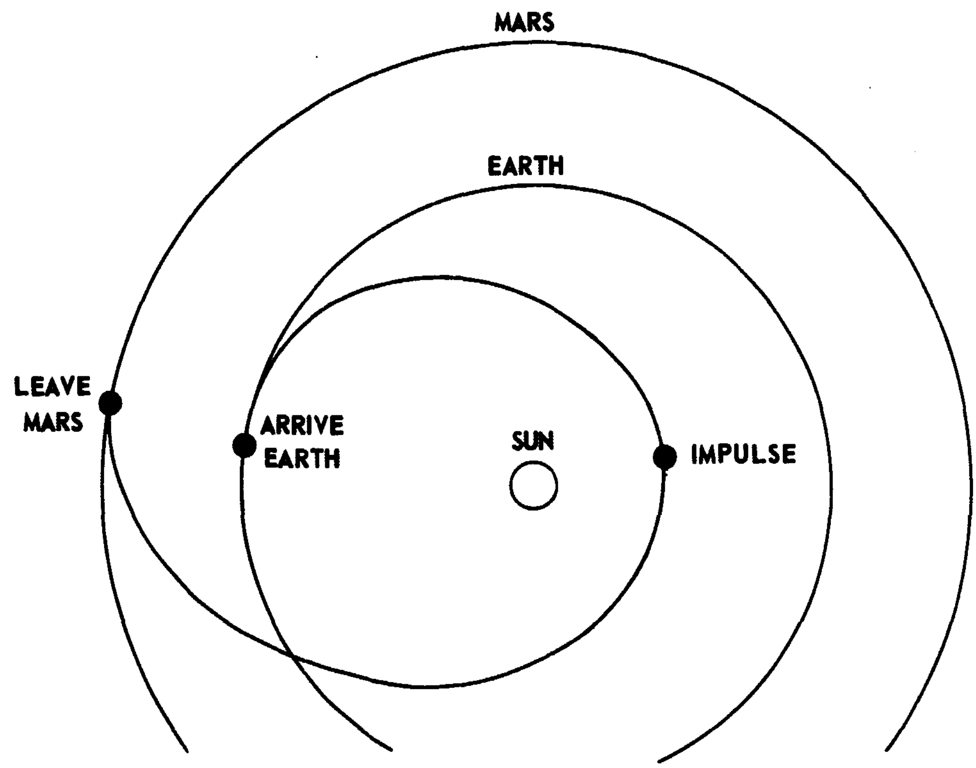

TWO IMPULSES

$\Delta V_T = 2.324$ EMOS

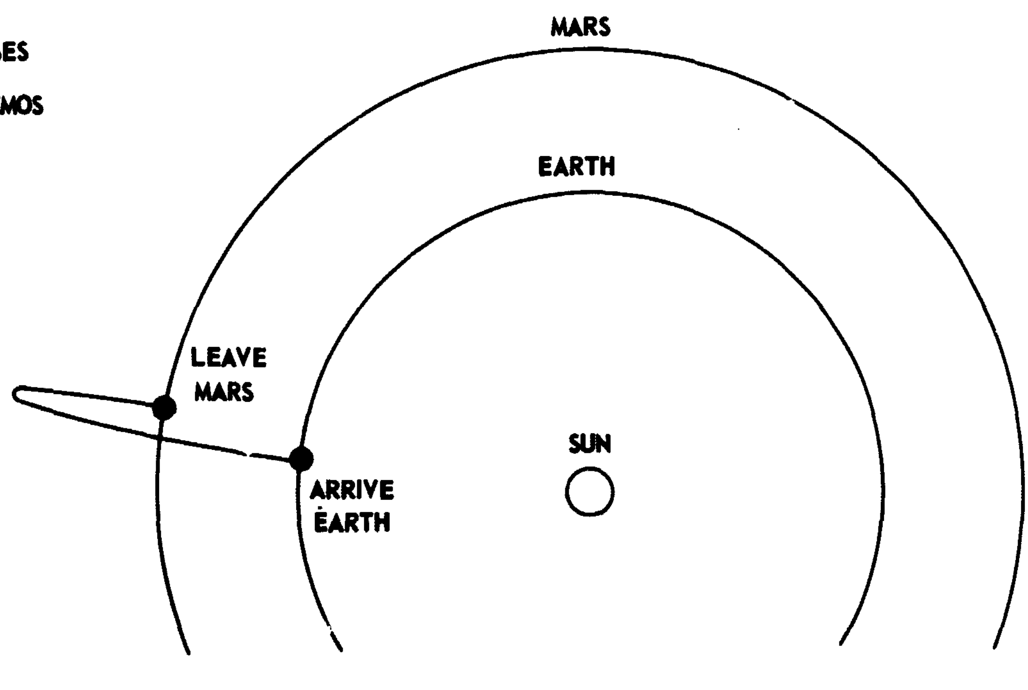

J-970850-7

FIG. 3

TYPICAL LOW-THRUST ACCELERATION HISTORIES
FIXED LAUNCH DATE

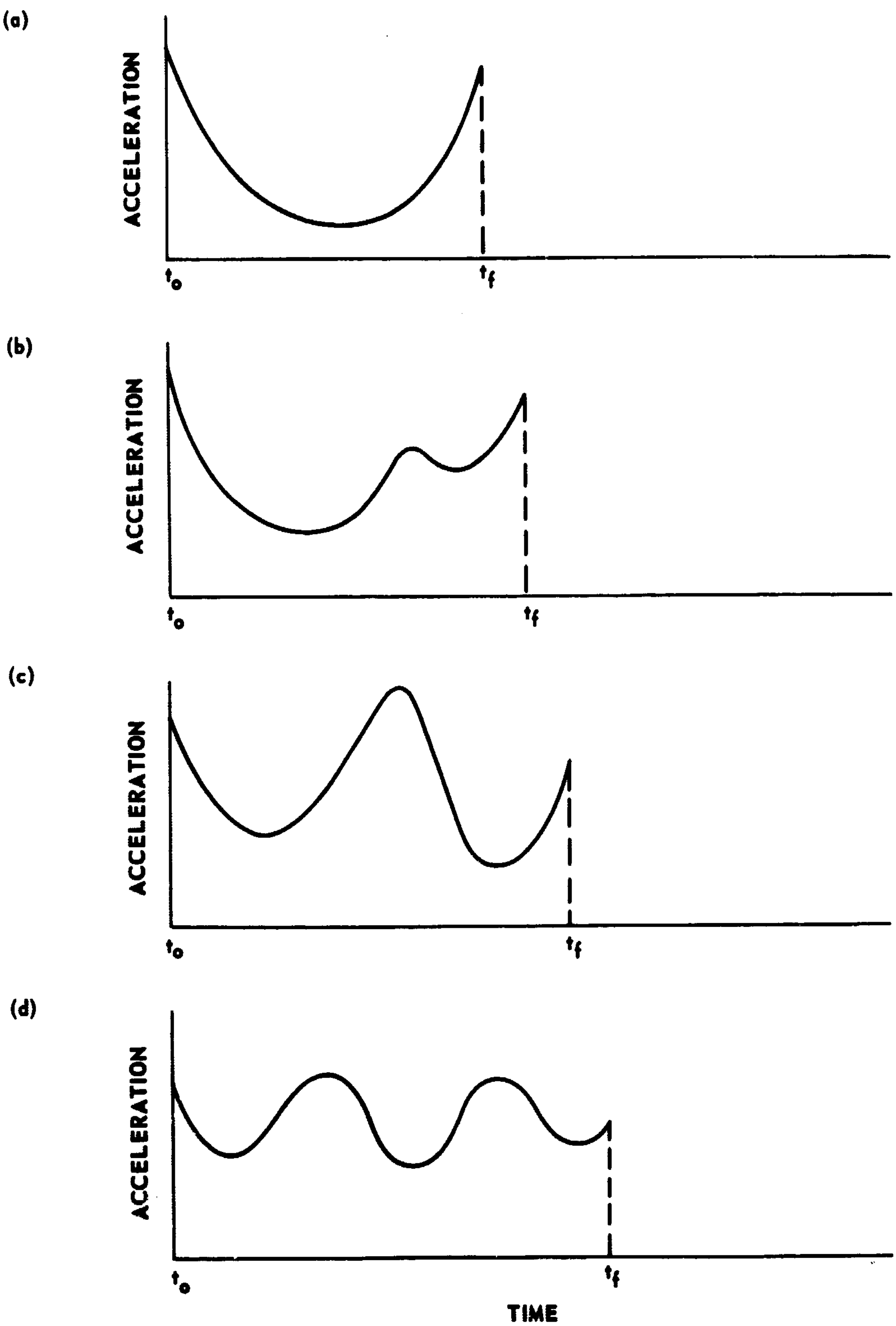

HOHMANN TRANSFER

$r_1 = 1.0$ AU
$r_2 = 1.5$ AU
$t = 255.58$ DAYS

$\Delta V_1 = 0.09536$ EMOS
$\Delta V_2 = 0.08626$ EMOS

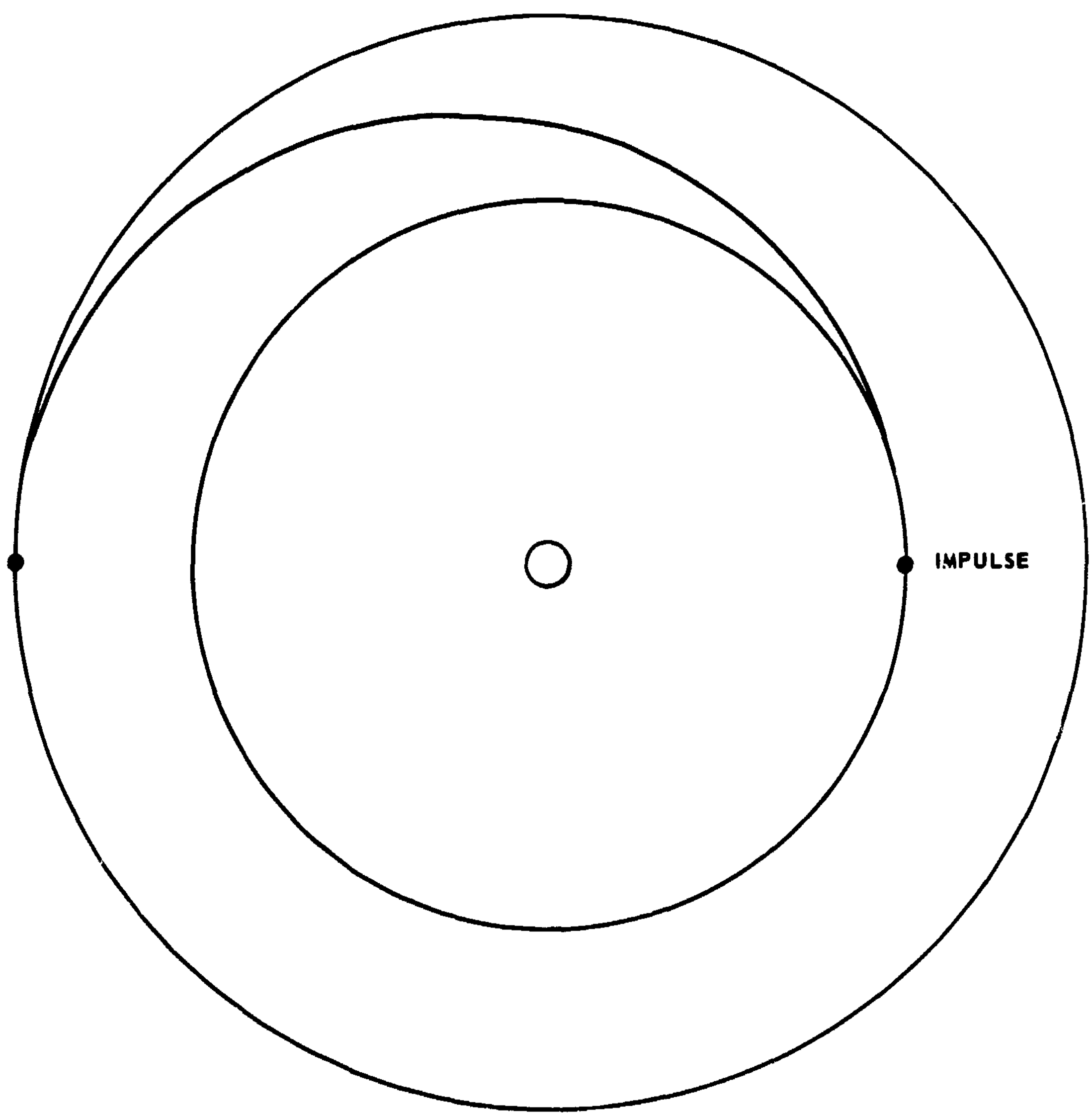

PRIMER MAGNITUDE HISTORY

HOHMANN TRANSFER

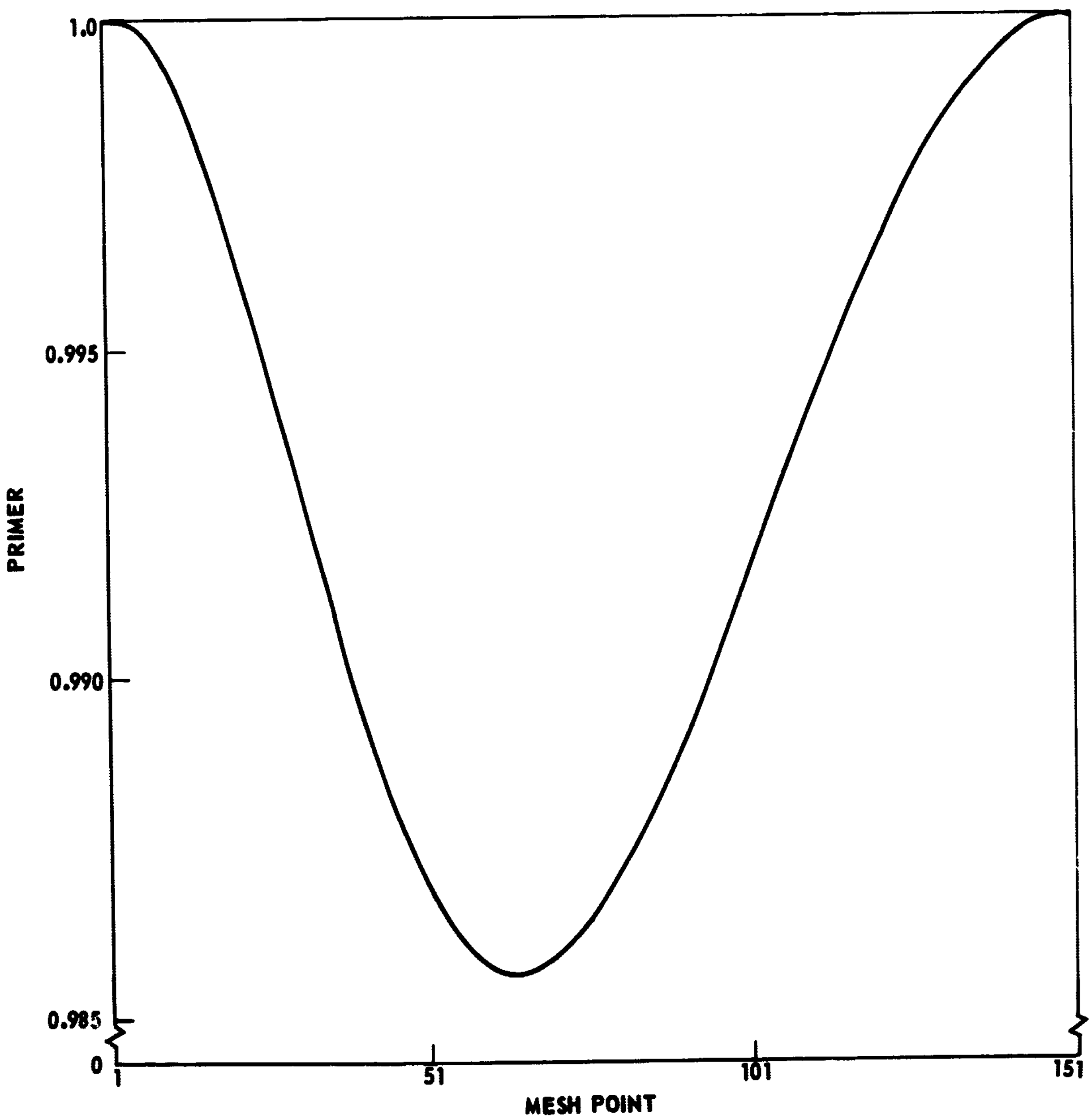

BIELLIPTIC TRANSFER

r_1 = 1.0 AU

r_2 = 1.5 AU

r_3 = 2.0 AU

t = 678.01 DAYS

ΔV_1 = 0.09555 EMOS

ΔV_2 = 0.14254 EMOS

ΔV_3 = 0.05234 EMOS

t_1 = 422.43 DAYS

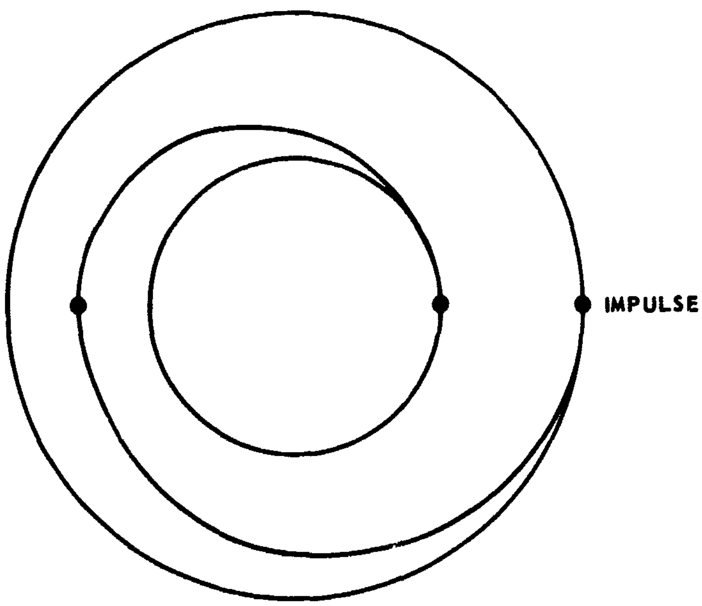

PRIMER MAGNITUDE HISTORY
BIELLIPTIC TRANSFER

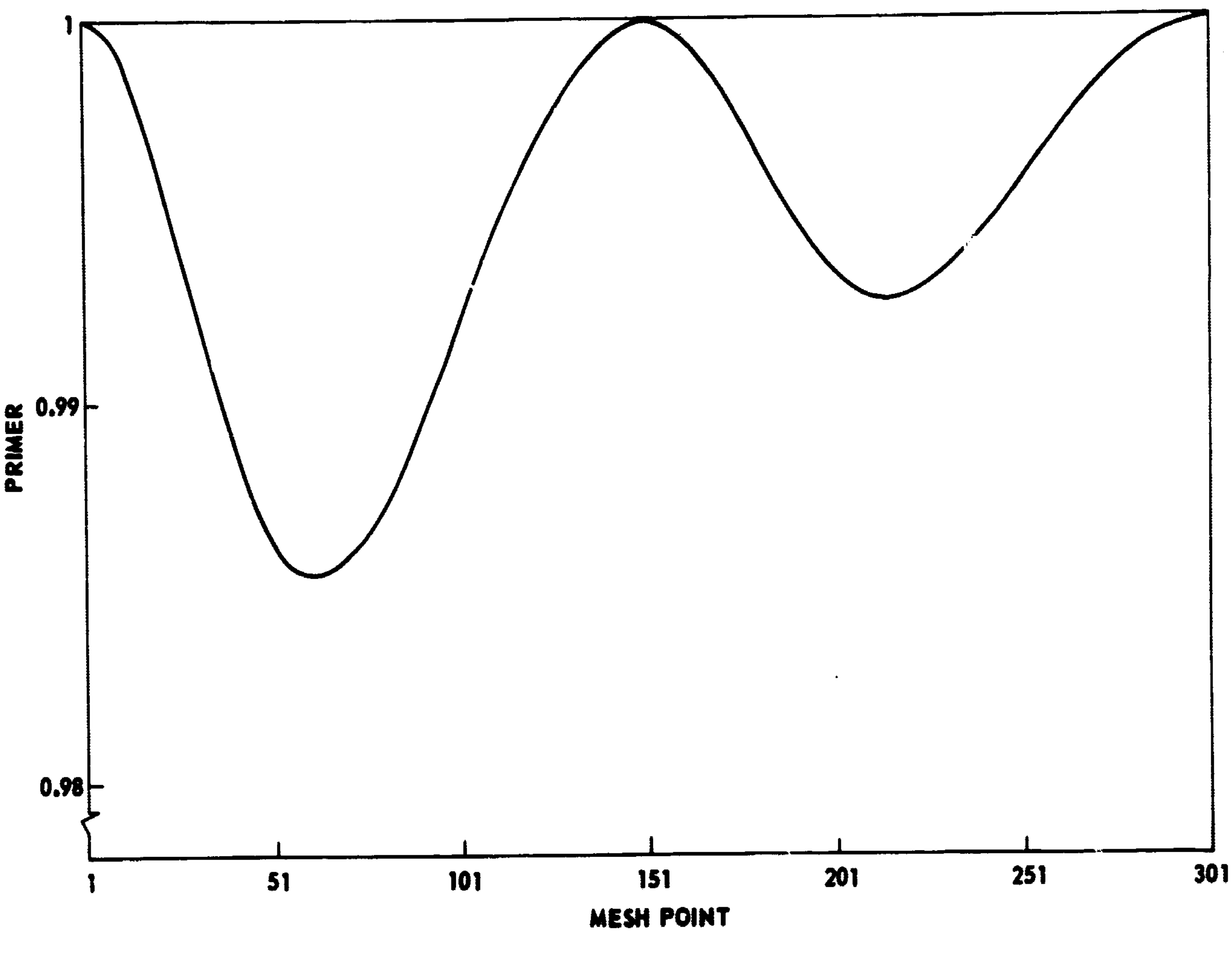

200-DAY COPLANAR EARTH-MARS RENDEZVOUS

2-IMPULSE

ΔV_1 = 0.28554 EMOS

ΔV_2 = 0.19630 EMOS

ΔV_{TOT} = 0.48184 EMOS

3-IMPULSE

ΔV_1 = 0.22108 EMOS

ΔV_2 = 0.04710 EMOS

ΔV_3 = 0.21087 EMOS

ΔV_{TOT} = 0.47905 EMOS

t_i = 48.2 DAYS

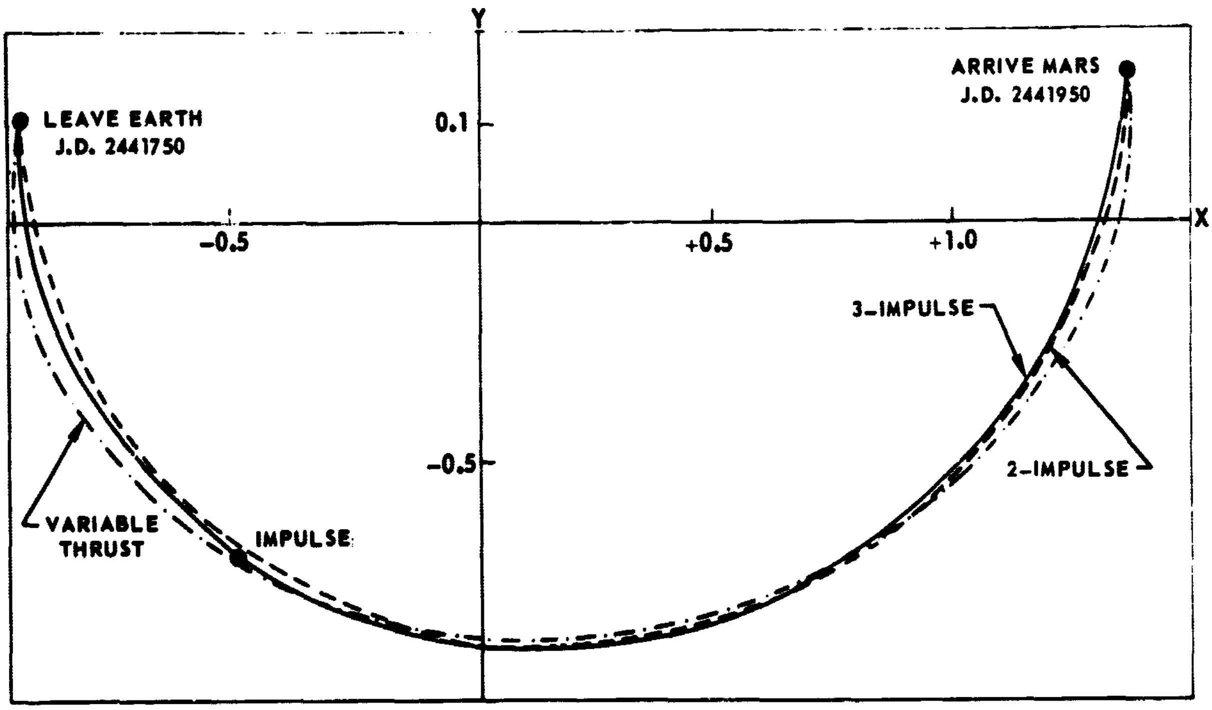

PRIMER MAGNITUDE HISTORIES
EARTH-MARS RENDEZVOUS

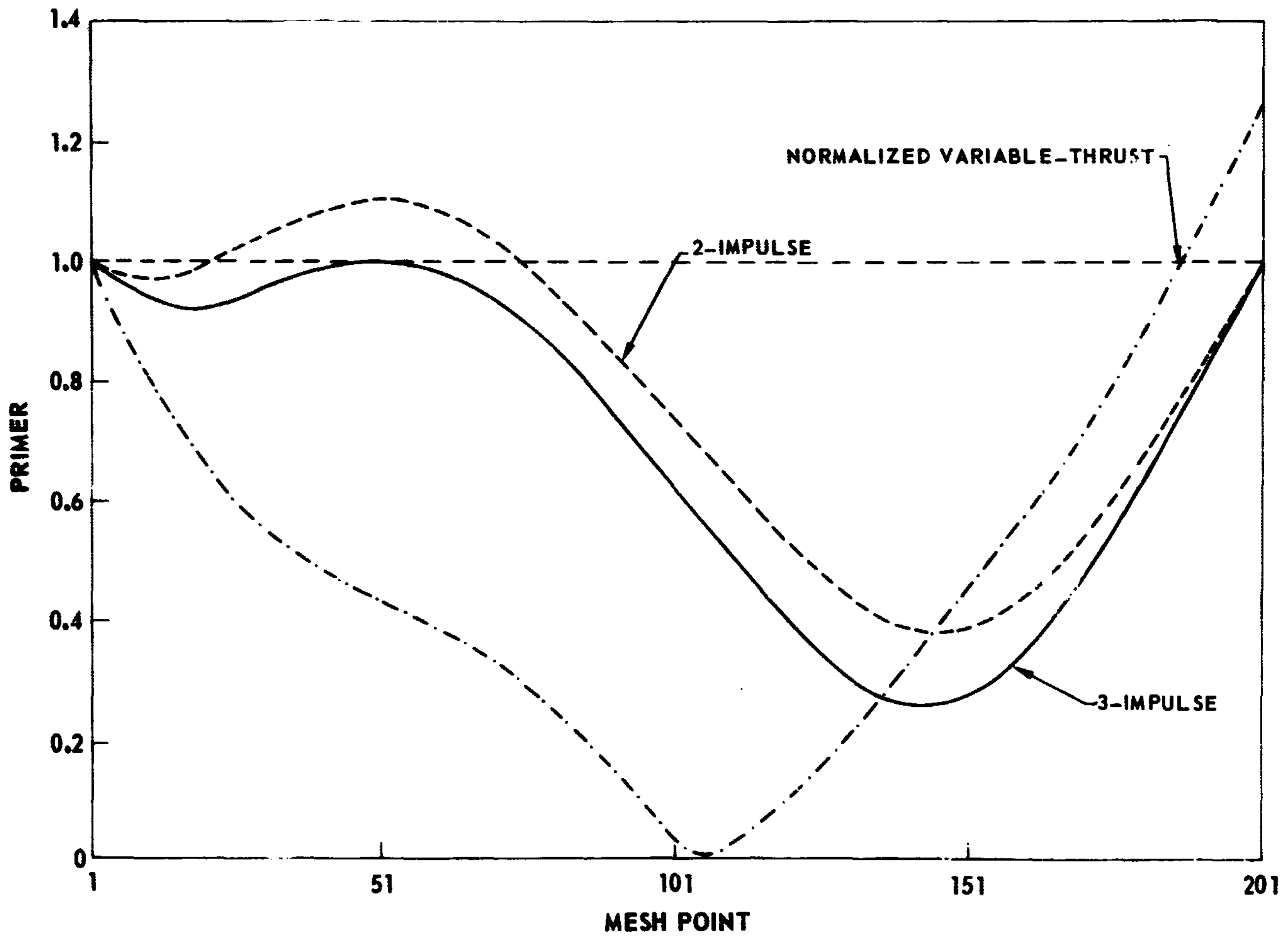

J-970850-7

FIG. 10

200-DAY MARS-EARTH RENDEZVOUS

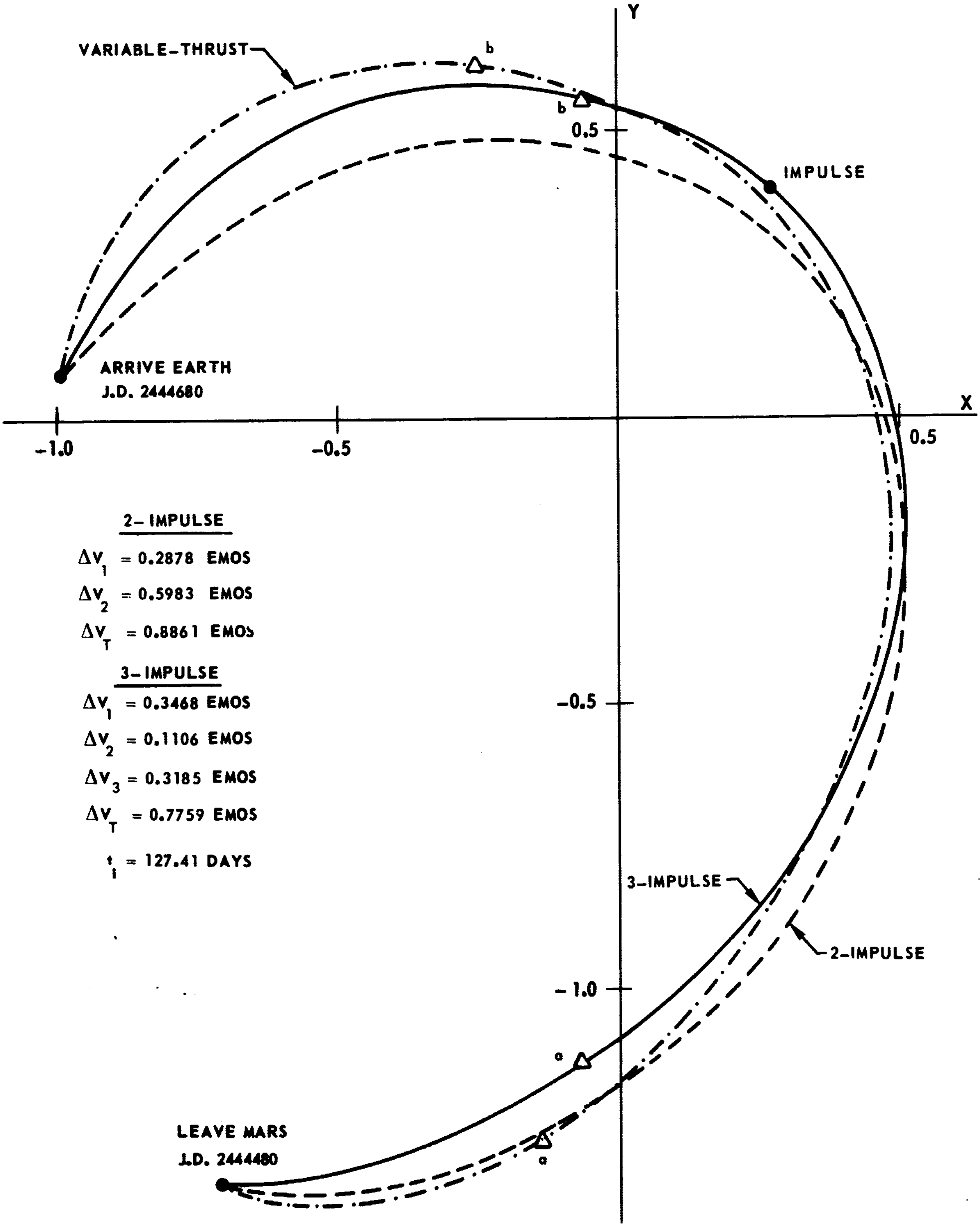

PRIMER MAGNITUDE HISTORIES
200-DAY MARS-EARTH RENDEZVOUS

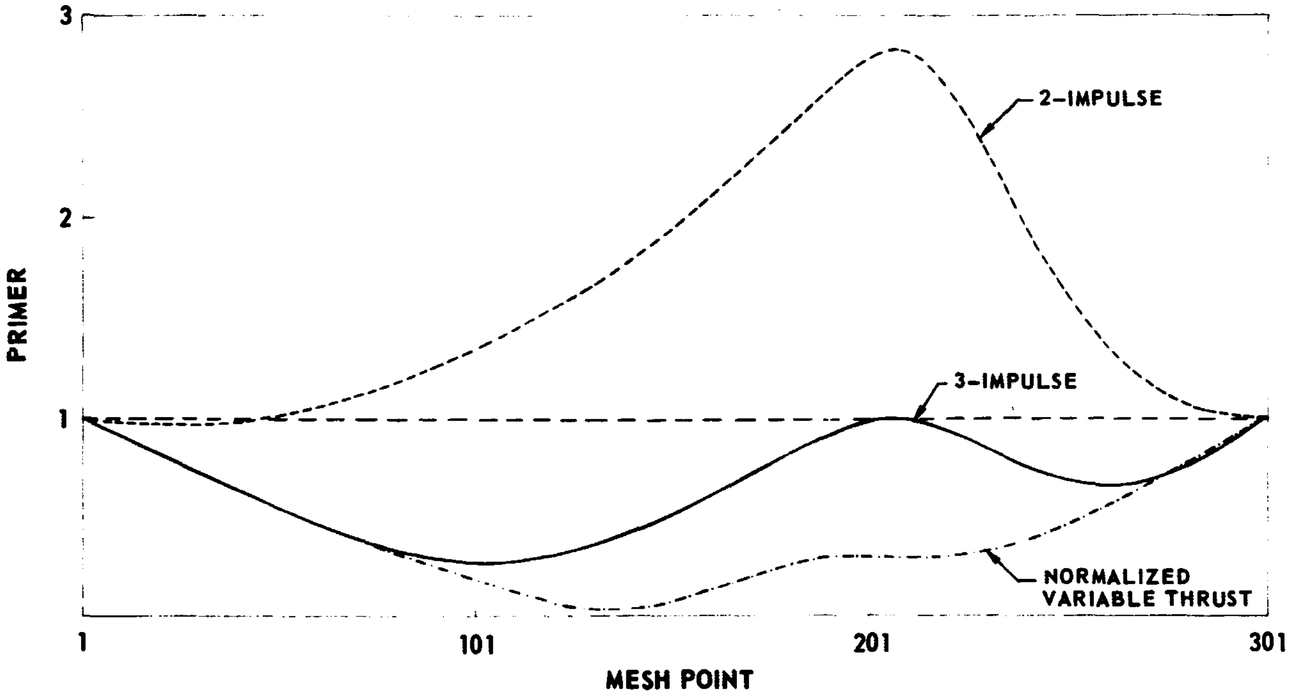

400-DAY CIRCLE-TO-CIRCLE RENDEZVOUS

r_1 = 1.0 AU

r_2 = 2.0 AU

2- IMPULSE

ΔV_1 = 0.4348 EMOS

ΔV_2 = 0.2052 EMOS

ΔV_T = 0.6400 EMOS

3- IMPULSE

ΔV_1 = 0.0253 EMOS

ΔV_2 = 0.1601 EMOS

ΔV_3 = 0.1528 EMOS

ΔV_T = 0.3382 EMOS

t_i = 123.66 DAYS

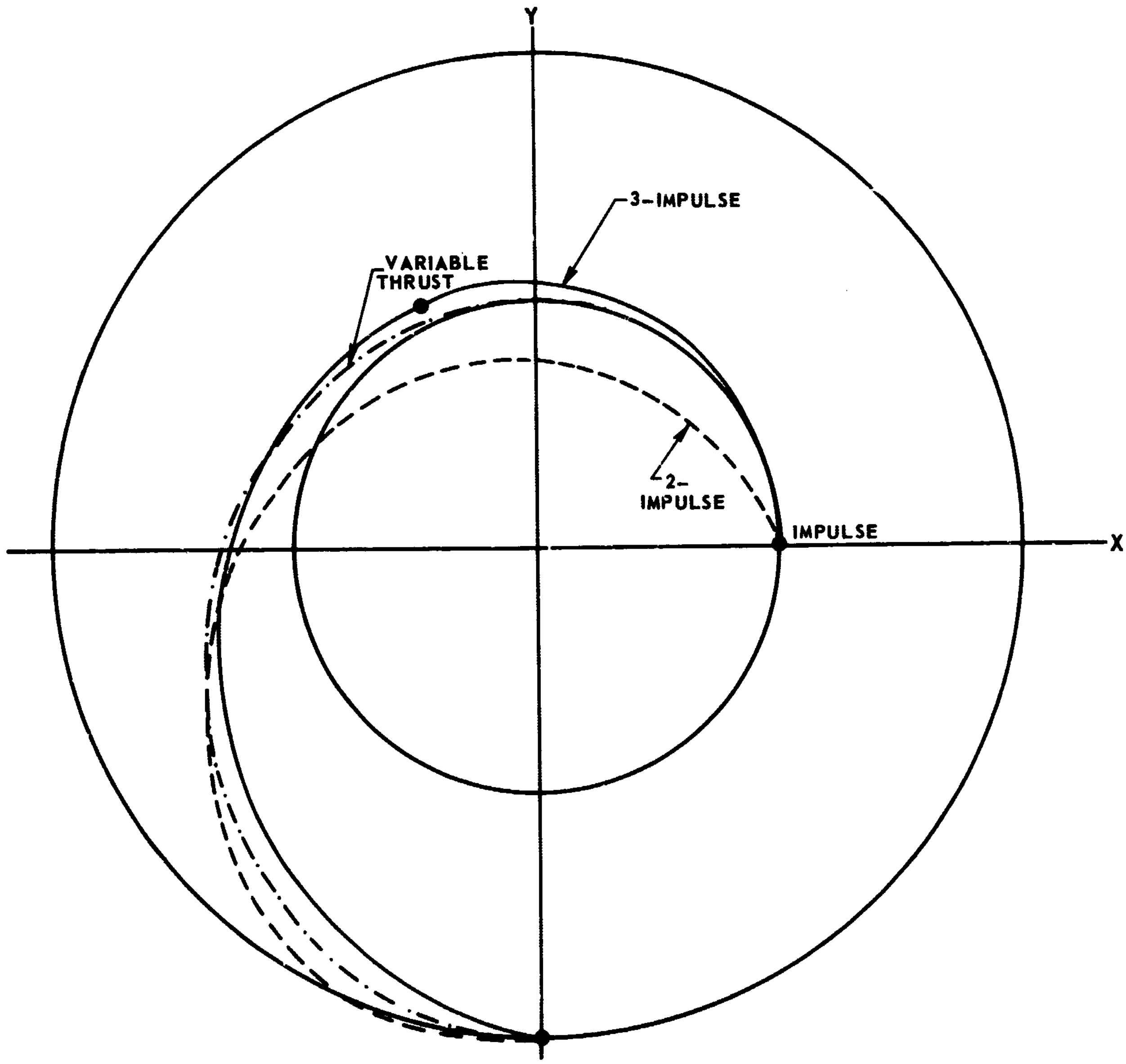

PRIMER MAGNITUDE HISTORIES
400-DAY CIRCLE-TO-CIRCLE RENDEZVOUS